Reporter Gene Assays

Cells cultured in 10- or 15-cm dishes in Dulbecco's modified Eagle medium containing 10% FBS were trypsinized. A quarter of the cells were lysed in 1 mL of passive lysis buffer (25 mmol/L Tris-phosphate [pH 7.8], 2 mmol/L dithiothreitol, 2 mmol/L 1,2-diaminocyclohexane-N,N,N′,N′-tetraacetic acid, 10% glycerol, and 1% Triton X-100). RL and FL activities were measured in 20 μL of cell lysate by using the Dual-Luciferase Reporter Assay System (Promega, Madison, WI). Total RNA was isolated from the remainder and processed for analysis by cDNA microarray, Northern blotting, and real-time detection (RTD) PCR.

Antisense Oligodeoxynucleotide

We designed respective antisense phosphorothioate oligos that were complementary to the sequence from 5 nts upstream to 15 downstream of the predicted translational initiation site of the La protein, PTB, eIF3 p170, eIF2γ, RNPL, poly(A)-binding protein, cytoplasmic 1 (PABPC-1), PCBP-2, and ribosomal protein S9 gene. The nt sequences of antisense oligos were 5′-GCCATTACGGCTATCTTTAA-3′ for La protein, 5′-TCCATGGCACACAGAGCAGA-3′ for PTB, 5′-GGCATTTTCCGGCCTCTGAA-3′ for eIF3 p170, 5′-CCAGCTTCTCCGCCCGCCAT-3′ for eIF2γ, 5′-ACCATCGCTCCCGACCGCCT-3′ for RNPL, 5′-TTCATCTCGGCACGGCTGCC-3′ for PABPC-1, 5′-TCCATGTCGAGCAGTGTTCT-3′ for PCBP-2, and 5′-GGCATGTTGCGTCCGCTTCCGCC-3′ for ribosomal protein S9. Positive and negative controls consisted of an antisense oligo for the 5′ region of HCV (nt 330–350), 5′-GTGCTCATGGTGCACGGTCT-3′,[29] and the randomized oligo, 6961, 5′-TACGTTTCTATGTCGATGGG-3′,[29] respectively. Oligodeoxynucleotides (0.5–1.0 μmol/L) were added to the medium by using the FuGENE6 transfection reagent (Boehringer Mannheim, Mannheim, Germany), and the cultures were incubated for 24 hours. Cells were harvested, and HCV IRES activity was evaluated by assaying the reporter genes. To validate repressed targeted gene expression, 1 μg of total RNA was amplified by RT-PCR with specific primers for La protein, PTB, eIF3 p170, and ribosomal protein S9. The internal control was the level of β-actin expression.

Synchronization of Cell Growth and Analysis of Cellular DNA Content

To examine the relationship between HCV IRES–directed translation and cell growth, RCF-26 cells and ΔRCF-9 cells were incubated in 15-cm dishes with low serum or at confluence for 24–48 hours. RCF-26 cells and ΔRCF-9 cells in 10-cm dishes were synchronized at the G_1/S phase border by starvation for 24 hours in medium containing 0.1% FBS, followed by a wash and an 18-hour incubation in medium containing 10% FBS and 2.5 μg/mL aphidicolin. Aphidicolin was removed from the synchronized cells by washing and adding fresh medium containing 1% FBS. The cells were harvested at 3-hour intervals over 48 hours to assess the cell-cycle phase and reporter enzyme activities. The cell-cycle phase distribution in each sample cell population was determined by measuring the DNA content of individual cells by flow cytometry.[22]

Complementary DNA Microarray Analysis

We profiled gene expression in cells at different phases of the cell cycle by cDNA microarray analysis. We reconstructed the gene set of cDNA microarray slides containing 1080 cDNA clones[30] by adding canonical and noncanonical initiation factors. The new microarray included La protein,[16] PTB,[18] eIF2β,[31] eIF2γ,[31] eIF3 p116, eIF3 p170,[32] RNPL,[19] ribosomal protein S9,[7] PCBP-2,[20] PABPC-1,[33] and cell division cycle 2–like 1 (PITSLRE proteins)[34] that bind HCV or other viral IRES structures and might affect the IRES activity. Other canonical initiation factors, such as eIF1A, eIF2A, eIF4A, eIF4B, eIF4E, and eIF5,[7,21,35] were also included to analyze cap-dependent translation machinery.

Total RNA (50 μg) isolated from serum-starved or confluent cells (10% FBS and at 60%–70% cell density) was labeled with a fluorescent dye for the cDNA microarray.[30,36,37] To profile gene expression in cells during the cell cycle, total RNA was periodically extracted from synchronized cells at 3, 9, 15, 18, 24, 30, 36, and 42 hours released from aphidicolin block (G_1/S border). After 1 round of amplification, antisense RNA was labeled and hybridized with the cDNA microarray.[30,36,37] Images were acquired, and cDNA microarray slides were analyzed as previously described.[30,36,37] A 1-dimensional self-organizing map (SOM) was constructed to cluster genes with a similar expression profile throughout cell-cycle progression (Cluster and Tree view; http://www.microarrays.org.html/software).

Northern Blotting

We evaluated La protein, PTB, and albumin expression in cultured cells and in tissue samples by Northern blotting. Total RNA (20 μg) was separated on denaturing agarose/formaldehyde gels, transferred to a membrane, and hybridized with specific probes under standard conditions.

Western Blotting

RCF-26 cells seeded in a 10-cm dish were grown to subconfluency and washed twice with phosphate-buffered saline. Cells were lysed in radioimmunoprecipitation assay buffer. Cell lysates were collected by pelleting cell debris, and the concentration of protein was quantified by using a dye-binding assay (Bio-Rad, Hercules, CA). Eighty micrograms of cell lysate was electrophoresed in a sodium dodecyl sulfate/12.5% polyacrylamide gel and electrotransferred to a nitrocellulose membrane. After blocking with phosphate-buffered saline with 0.3% Tween-20 containing 5% skim milk for 1 hour, the membranes were reacted with appropriate antibodies. After washing with phosphate-buffered saline with 0.3% Tween-20, membranes were reacted with horseradish peroxidase–conjugated anti-mouse immunoglobulin G or anti-rab-

bit immunoglobulin G antibodies diluted 1:3000. Membranes were washed again and then visualized with an enhanced chemiluminescence kit (Amersham Pharmacia Biotech, Uppsala, Sweden).

Real-Time Detection Polymerase Chain Reaction

The PCR reaction mixture was prepared by using TaqMan Universal Master Mix (PE Applied Biosystems, Foster City, CA). The primer set applied to amplify La protein messenger RNA (mRNA) consisted of 5′-CGCTGGGAGGTGGAGTCGTT-3′ (exon 1) and 5′-CCCGTGGCAAATTGAAGTCG-3′ (exon 2). The probe, 5′-TGCCCTGGAGGCCAAAATCTGTCATC-3′ (exon 2), was designed to target an internal region between the forward and reverse primers. The primer set for PTB mRNA was 5′-AGCACGCCAAGCTGTCGCT-3′ (exon 8) and 5′-GGAACGGAAAGGCCGAAGG-3′ (exons 8–10). The probe was 5′-ACACACGCCCAGACCTGCCTTCCG-3′ (exon 8). The primer set for eIF3 p170 protein mRNA was 5′-CCGGAAAATGCCCTCAAACTA-3′ (exon 1) and 5′-AAGTGGCTCTTGCGAAGATCCACGC-3′ (exon 7). The probe sequence was 5′-CCAACGAATTTCTTGAGGTT-3′ (exon 2). The primer set for the internal control glyceraldehyde-3-phosphate dehydrogenase mRNA was designed according to GenBank M33197 by using the following primers: exon 7, 5′-TGCACCACCAACTGCTTAGCACCC-3′; and exon 8, 5′-CTTGATGTCATCATATTTGGCAGG-3′. The probe for glyceraldehyde-3-phosphate dehydrogenase-P, designed on the basis of exons 7 and 8, was 5′-TGACCACAGTCCATGCCATCACTGC-3′. Fifty PCR amplification cycles of 95°C for 30 seconds, 60°C for 40 seconds, and 72°C for 30 seconds were repeated by using a real-time PCR system (ABI PRISM 7700 Sequence Detection System; PE Applied Biosystems). To prepare standard RNA, PCR products were cloned into pBluescript vector and linearized at the T3 promoter site. Standard RNA was synthesized by using T7 RNA polymerase and purified by using Isogen (Wako Junyaku, Osaka, Japan) and deoxyribonuclease I (TaKaRa, Shiga, Japan). We detected HCV RNA in liver by using RTD-PCR as previously described.[38]

Statistical Analysis

All data are expressed as means ± SEM. Significance was tested by the Student *t* test and 1-way analysis of variance with Bonferroni's methods.

Results

Gene-Expression Profiling in Confluent or Serum-Starved Cells and the Activities of Hepatitis C Virus Internal Ribosomal Entry Site–Directed Translation

RCF-26 cell lines constitutively express dicistronic RNA transcripts containing sequences encoding the reporter proteins RL and FL separated by a functional HCV IRES (Figure 1). The activities of these proteins expressed in RCF-26 cells reflect cap-dependent and HCV IRES–directed translation, respectively. To rule out the possibility that FL activity from the second cistron reflected the nonspecific ribosomal scanning rather than HCV IRES–directed translation, we evaluated RL and FL activities in ΔRCF-9 cells in which the functional HCV IRES element had been deleted. The ratio of FL to RL (relative HCV IRES activity) in ΔRCF-9 was 2.5% of that in RCF-26, thus reflecting the specificity of HCV IRES activity in RCF-26 cells (Figure 2*B–D*).

To examine the relationship of the cellular proteins that vary in abundance and HCV IRES activities, RCF-26 cells and ΔRCF-9 cells were cultured in 15-cm dishes at confluence or under serum depletion for 48 hours, and changes in cellular gene expression and HCV IRES activities were evaluated. Under these conditions, the cellular DNA content increased at G_0/G_1 phase (49% to 74% in confluent cells and to 59% in serum-starved cells) and decreased at S phase (38% to 18% in confluent cells and to 35% in serum-starved cells) or G_2/M phase (14% to 8% in confluent cells and to 6% in serum-starved cells; Figure 2*A*). The degree of changes during the cell cycle was much greater in the confluent cells than in the serum-starved cells. The activities of HCV IRES–directed translation were reduced to 24% in confluent cells and to 22% in serum-starved cells compared with controls (Figure 2*C* and *D*), whereas the activities of cap-dependent cellular translation were essentially maintained (Figure 2*B*). Neither a significant difference in FL activity nor relative HCV IRES activity was found in ΔRCF-9 under these conditions (Figure 2*C* and *D*).

These results were not due to variations in the RNA stability of the RL and FL reporter genes. Northern blotting of mRNA transcribed from dicistronic constructs containing sequences encoding these 2 reporter proteins did not show either RNA degradation or splicing (data not shown). The relative expression ratio of mRNA of RL to FL determined by cDNA microarray did not change in either confluent or serum-starved cells (Figure 2*E*).

Gene-expression profiling changed in response to these conditions listed in Table 1. Serum proteins such as α_2-macroglobulin and albumin, as well as cell adhesion molecules such as cadherin, major histocompatibility complex, and fibronectin, were up-regulated by more than 1.8-fold. Albumin, a major serum protein that is specifically produced in the liver, was remarkably regulated in a cell-cycle dependent manner. However, cell-cycle and growth-related genes such as cyclin A, cyclin B, CDK1, cell division cell cycle 18, p53, hepatoma-

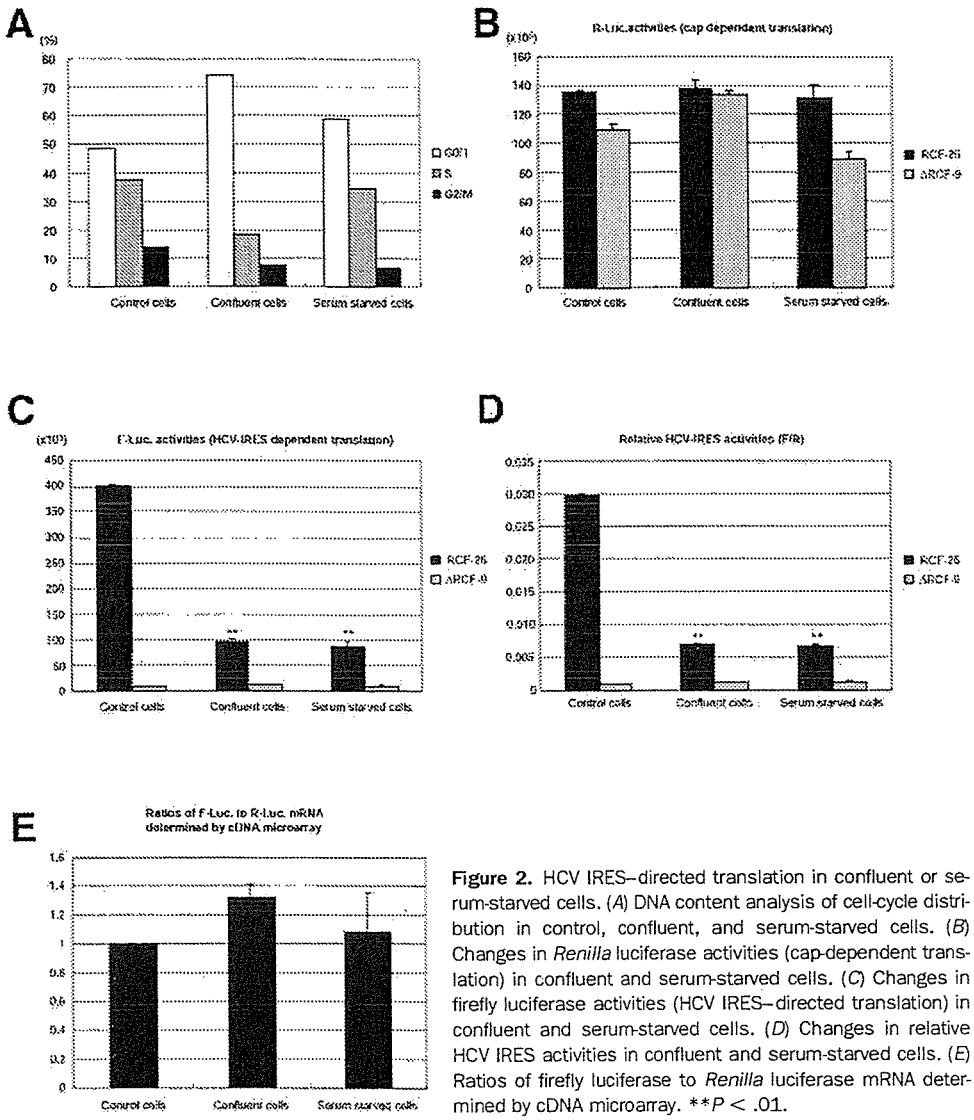

Figure 2. HCV IRES–directed translation in confluent or serum-starved cells. (*A*) DNA content analysis of cell-cycle distribution in control, confluent, and serum-starved cells. (*B*) Changes in *Renilla* luciferase activities (cap-dependent translation) in confluent and serum-starved cells. (*C*) Changes in firefly luciferase activities (HCV IRES–directed translation) in confluent and serum-starved cells. (*D*) Changes in relative HCV IRES activities in confluent and serum-starved cells. (*E*) Ratios of firefly luciferase to *Renilla* luciferase mRNA determined by cDNA microarray. $^{**}P < .01$.

derived growth factor, and nm23 were down-regulated, as were genes related to RNA polymerase, such as RNA polymerase II, subunit 5-mediating protein (RMP), La protein, and topoisomerase II. The La protein binds the stem loop IV structure in HCV IRES and stimulates HCV IRES–directed translation.[16,17] With regard to changes in the expression of canonical and noncanonical initiation factors (Table 2), La protein and PTB expression were repressed in both confluent and serum-starved cells. The expression of eIF3 (p170 and p116) was predominantly repressed in confluent cells, and the expression of eIF2γ was predominantly repressed in serum-starved cells. Conversely, the expression of ribosomal protein S9 and PABPC-1 was induced in confluent cells. The degree to which gene expression changed was more predominant in confluent cells than in serum-starved cells. This might reflect the greater degree of changes in the cell-cycle distribution of G_0/G_1 and S phases in confluent cells than in serum-starved cells (Figure 2*A*). The results of northern blots of La protein, PTB, and albumin expression coincided with these results (Figure 3). We evaluated changes in La protein and PTB expression by using RTD-PCR. The relative expression of La protein in confluent and serum-starved cells was 16% and 33% of control cells, respectively. The relative expression of PTB in confluent and serum-starved cells was 10% and 26% of control cells, respectively (data not shown). These data suggest that several canonical and noncanonical initiation factors, such as La protein, PTB, eIF3, and eIF2γ, are initiation factors responsible for regulating HCV IRES activity in a cell cycle–dependent manner.

Table 1. Up- and Down-regulated Genes in Confluent and Serum-Starved Cells

UniGene	Gene name	Category	Confluent cells	Serum-starved cells	Mean (fold)
Up-regulated					>1.8
Hs.74561	Alpha-2-macroglobulin	Serum protein	12.87 ± 2.13	5.13 ± 0.10	9.00 ± 2.40
Hs.75442	Albumin	Serum protein	6.07 ± 1.07	3.26 ± 0.37	4.67 ± 0.93
Hs.77054	B-cell translocation gene 1	Antiproliferative gene	4.73 ± 1.76	2.97 ± 0.83	3.85 ± 0.94
Hs.82004	Cadherin 1, E-cadherin (epithelial)	Cell adhesion	5.14 ± 2.46	2.36 ± 0.30	3.75 ± 1.29
Hs.2257	Vitronectin	Cell adhesion	3.97 ± 0.68	2.11 ± 0.22	3.04 ± 0.61
Hs.277477	MHC class IC	Cell adhesion	3.26 ± 0.82	2.17 ± 0.09	2.71 ± 0.46
Hs.77961	MHC class IB	Cell adhesion	3.33 ± 0.23	2.08 ± 0.24	2.71 ± 0.39
Hs.1119	TR3 orphan receptor	Receptor	3.38 ± 1.23	1.95 ± 0.23	2.66 ± 0.66
Hs.1665	Zinc finger transcriptional regulator	Transcription factor	2.66 ± 0.40	2.53 ± 0.40	2.60 ± 0.23
Hs.287820	Fibronectin gene	Cell adhesion	2.40 ± 0.77	2.11 ± 0.34	2.26 ± 0.36
Hs.2780	JunD	Oncogene	2.23 ± 0.39	1.99 ± 0.54	2.11 ± 0.28
Down-regulated					<0.55
Hs.89525	Hepatoma-derived growth factor	Cell growth	0.67 ± 0.27	0.42 ± 0.08	0.55 ± 0.13
Hs.7943	RMP	RNA polymerase II binding	0.44 ± 0.09	0.64 ± 0.07	0.54 ± 0.07
Hs.23960	Cyclin B	Cell cycle	0.44 ± 0.25	0.62 ± 0.17	0.53 ± 0.13
Hs.118638	Nm23A	Cell growth	0.52 ± 0.01	0.53 ± 0.11	0.52 ± 0.05
Hs.83715	Autoantigen La	RNA polymerase III synthesis	0.43 ± 0.06	0.61 ± 0.01	0.52 ± 0.06
Hs.16297	COX17	Cytochrome-*c*-oxidase	0.47 ± 0.14	0.55 ± 0.06	0.51 ± 0.07
Hs.95577	CDK1	Cell cycle	0.36 ± 0.02	0.65 ± 0.07	0.50 ± 0.09
Hs.174017	Topoisomerase (DNA) II alpha	RNA polymerase II holoenzyme	0.44 ± 0.11	0.55 ± 0.08	0.50 ± 0.05
Hs.85137	Cyclin A	Cell cycle	0.42 ± 0.03	0.56 ± 0.17	0.49 ± 0.08
Hs.9235	Nucleoside-diphosphate kinase	Cell growth	0.51 ± 0.08	0.46 ± 0.05	0.49 ± 0.04
Hs.75133	Transcription factor 6–like 1	Transcription factor	0.40 ± 0.07	0.57 ± 0.18	0.48 ± 0.09
Hs.69563	Cell division cycle 18	Cell cycle	0.45 ± 0.04	0.51 ± 0.09	0.48 ± 0.04
Hs.58593	RAP30	Transcription factor	0.37 ± 0.02	0.58 ± 0.00	0.48 ± 0.06
Hs.75323	Prohibitin	Antiproliferative gene	0.50 ± 0.01	0.39 ± 0.01	0.44 ± 0.03
Hs.1846	p53	Cell cycle	0.66 ± 0.18	0.22 ± 0.04	0.44 ± 0.15
Hs.111758	Keratin 6	Housekeeping	0.24 ± 0.02	0.63 ± 0.07	0.43 ± 0.12
Hs.78271	Keratin 8	Housekeeping	0.33 ± 0.18	0.53 ± 0.08	0.43 ± 0.10
Hs.748	Fibroblast growth factor receptor 1	Cell growth	0.39 ± 0.12	0.30 ± 0.05	0.34 ± 0.06

Hepatitis C Virus Internal Ribosome Entry Site Activity at Different Phases of the Cell Cycle

We examined the relationship between HCV IRES activity and cell division in more detail. We synchronized cell-cycle progression and compared the production of RL and FL reporter proteins during different phases of the cell cycle. Cells were blocked at the G_1/S interface by adding aphidicolin to the culture medium and were then released from the aphidicolin

Table 2. Up- and Down-regulated Initiation Factors in Confluent and Serum-Starved Cells

UniGene	Gene name	Confluent cells	Serum-starved cells	Mean (fold)
Hs.180920	Ribosomal protein S9	1.92 ± 0.01	1.11 ± 0.18	1.51 ± 0.24
Hs.172550	Polypyrimidine tract binding protein (PTB)	0.62 ± 0.17	0.62 ± 0.03	0.62 ± 0.07
Hs.83715	La protein	0.43 ± 0.06	0.61 ± 0.01	0.52 ± 0.06
Hs.2730	Heterogeneous nuclear ribonucleoprotein L (RNPL)	1.23 ± 0.33	1.02 ± 0.13	1.13 ± 0.16
Hs.63525	Poly(rC)-binding protein 2 (PCBP2)	1.20 ± 0.11	0.95 ± 0.10	1.07 ± 0.09
Hs.172182	Poly(A)-binding protein, cytoplasmic 1	1.87 ± 0.62	1.19 ± 0.05	1.53 ± 0.32
Hs.183418	Cell division cycle 2–like 1 (PITSLRE proteins)	0.85 ± 0.10	0.70 ± 0.07	0.78 ± 0.07
Hs.198899	eIF3-p170	0.47 ± 0.28	1.10 ± 0.36	0.79 ± 0.26
Hs.57783	eIF3-p116	0.58 ± 0.12	0.70 ± 0.02	0.64 ± 0.06
Hs.4310	eIF1A	0.84 ± 0.06	0.89 ± 0.17	0.86 ± 0.07
Hs.151777	eIF2A	1.37 ± 0.20	1.59 ± 0.20	1.48 ± 0.13
Hs.12163	eIF2β	0.88 ± 0.10	0.94 ± 0.02	0.91 ± 0.04
Hs.211539	eIF2γ	1.31 ± 0.03	0.61 ± 0.17	0.96 ± 0.22
Hs.129673	eIF4A	1.05 ± 0.09	0.81 ± 0.07	0.93 ± 0.08
Hs.93379	eIF4B	1.38 ± 0.48	0.94 ± 0.20	1.16 ± 0.25
Hs.79306	eIF4E	0.86 ± 0.14	0.83 ± 0.01	0.84 ± 0.06
Hs.286236	eIF5	0.91 ± 0.02	1.23 ± 0.35	1.07 ± 0.17

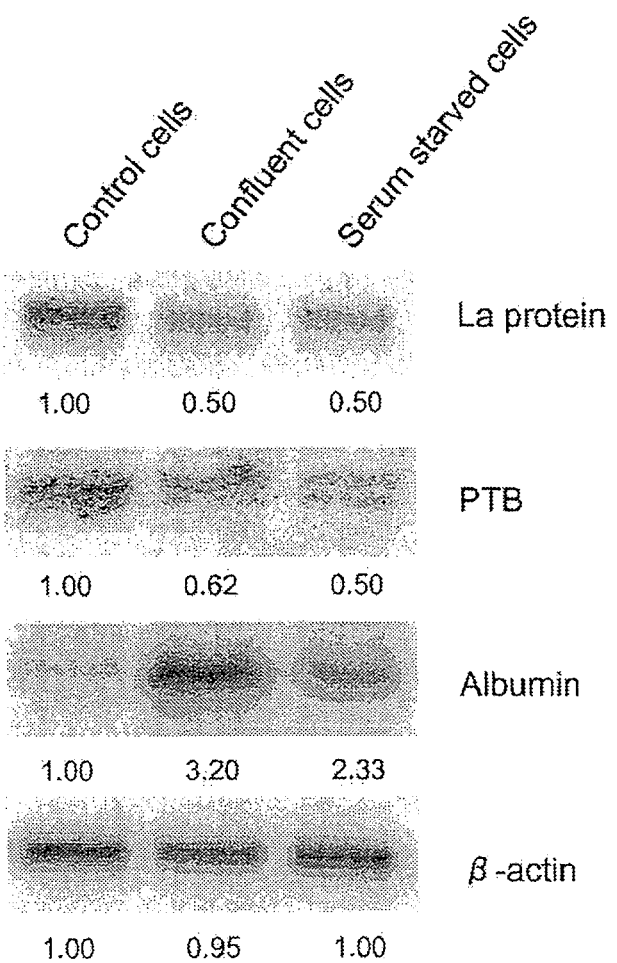

Figure 3. Northern blotting of La protein, PTB, and albumin in RCF-26. Expression of La protein and PTB is repressed in confluent and serum-starved cells, whereas albumin expression is significantly up-regulated.

block. Synchronized cells subsequently moved into the S and G_2/M phases of the cell cycle and then returned to G_1/S phase at approximately 27 hours, as determined by the cellular DNA content measured by flow cytometry (Figure 4*A*). RL activities increased proportionally, reflecting the increased number of cells after division. The cell number doubled at approximately 27 hours after 1 round of the cycle was completed. Conversely, HCV IRES activity varied with cell cycle, and the ratio of FL to RL (relative HCV IRES activity) increased during and immediately after G_2/M phase (12–18 hours after release from aphidicolin). The relative HCV IRES activity decreased by 36 hours after release (Figure 4*C*), corresponding to reentry into the G_0 and G_1 phases. However, the HCV IRES activity increased again, starting at approximately 39 hours, probably because many cells continued into a second cycle (Figure 4*A* and *C*). No significant differences in relative HCV IRES activity were found in ΔRCF-9 cells up to 30 hours after release (Figure 4*C*).

Gene-Expression Profiles in Cells Undergoing Cell-Cycle Progression

To determine which host factors are involved in this cell cycle–dependent regulation of HCV IRES activity, we evaluated gene-expression profiles in cells undergoing cell-cycle progression. Total RNA was extracted from synchronized cells at 3, 9, 15, 18, 24, 30,

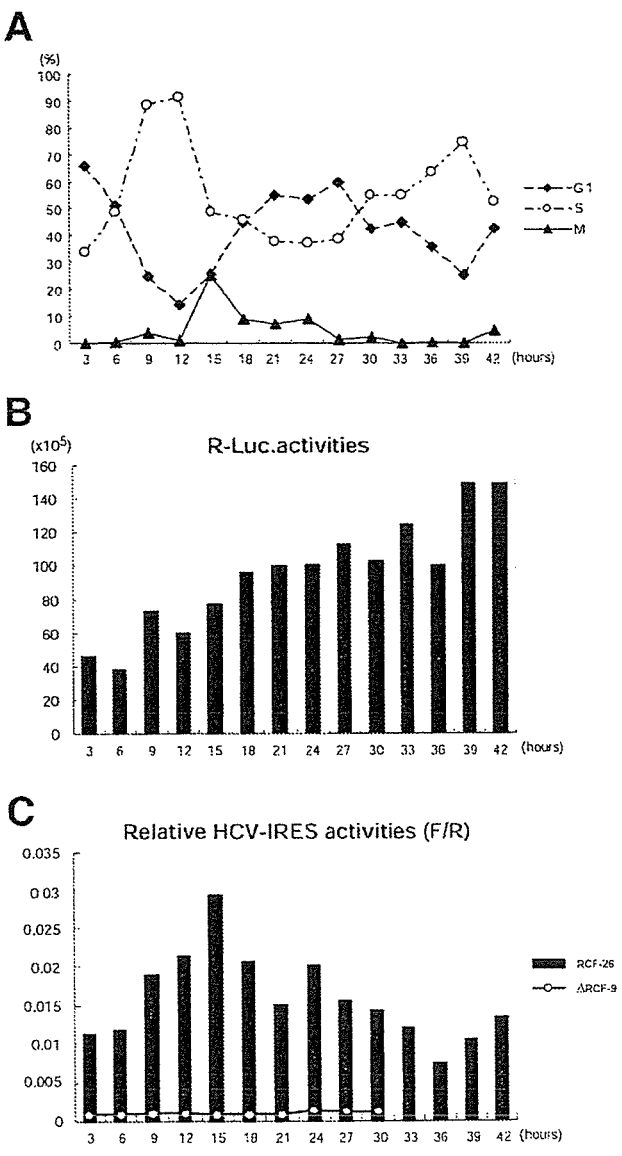

Figure 4. HCV IRES activity and cell-cycle progression. (*A*) Changes in distribution with cell-cycle progression. Proportions of G_1, S, and G_2/M are individually shown. (*B*) Changes of *Renilla* luciferase activities (cap-dependent translation) with cell-cycle progression. (*C*) Changes in relative HCV IRES activities (firefly to *Renilla* luciferase activities; FL/RL) with cell-cycle progression. HCV IRES activity varied with cell cycle in RCF-26 cells but did not change in ΔRCF-9 cells.

36, and 42 hours after release from the aphidicolin block (G_1/S border) and was analyzed with the cDNA microarray. We constructed a 1-dimensional SOM to evaluate changes in gene expression (Cluster and Tree view; http://www.microarrays.org/software/html) (Figure 5). We identified 3 large gene clusters as the cell cycle progressed. The first cluster of genes was induced at S phase (at 3 to 9 hours). The second and third clusters were induced at G_2/M (at 15–18 hours) and at G_1 (at 24 to 36 hours), respectively. Most of the HCV IRES–related canonical and noncanonical initiation factors were induced during S and G_2/M phases. PCBP-2, PTB, eIF3 (p110 and p170), eIF2γ, and eIF2β were induced during S phase, whereas La protein and RNPL were induced during G_2/M. These factors bind HCV IRES structure or have functional relevance to HCV IRES activity. Conversely, PABPC-1, eIF4A, and eIF4B were induced during G_1 phase. These factors are not required for HCV IRES–directed translation but are necessary for cap-dependent translation.[39] The induction of the ribosomal protein S9 in G_1 phase was a controversial finding because S9 was reported to bind stem loop IIId of HCV IRES. The functional role of the ribosomal protein S9 is discussed later. In cells, translation takes place immediately in the presence of mRNA, and luciferase activity could be detected within 30 seconds from the initiation of the translation. Thus, the induction of canonical and noncanonical initiation factors related to HCV IRES during S and G_2/M phases contributed to cell cycle–dependent regulation of translation directed by HCV IRES (Figure 5).

We evaluated changes in La protein expression determined by the cDNA microarray by using RTD-PCR (Figure 6). The changes in HCV IRES–directed translation and in La protein expression closely correlated (Figure 6).

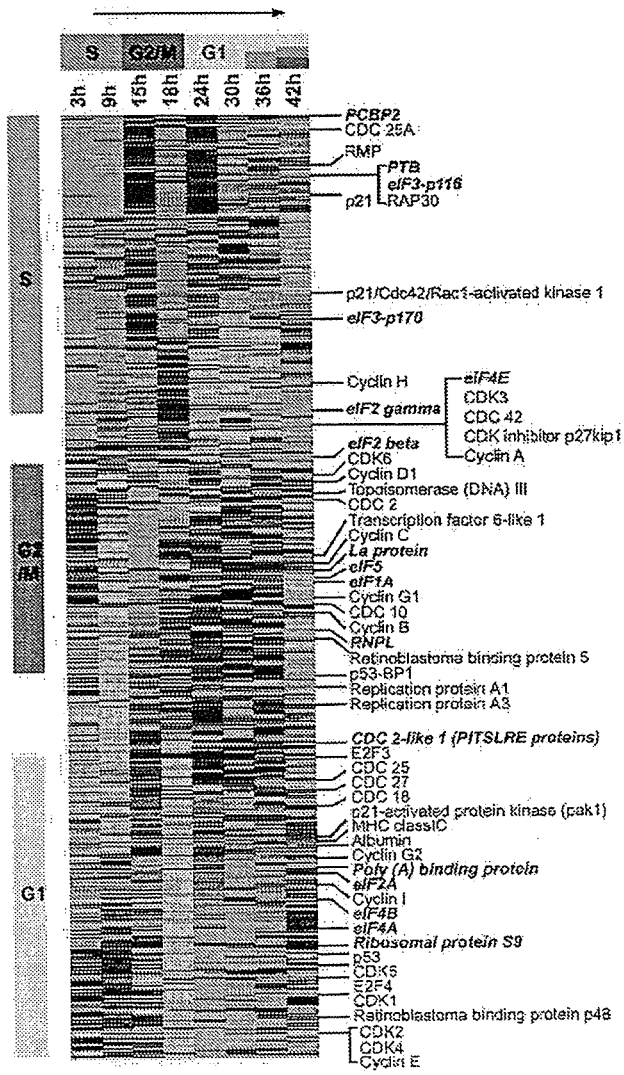

Figure 5. Gene-expression profiling in RCF-26 cells undergoing cell-cycle progression. RCF-26 cells were synchronized at the G_1/S border with aphidicolin. After release from aphidicolin block, the cell cycle progressed to S phase at 3–6 hours and G_2/M phase at 15–18 hours and returned to G_1 phase at 24–30 hours. Cells were harvested at 3, 9, 15, 18, 24, 30, 36, and 42 hours and analyzed with cDNA microarray, and then an SOM was constructed by using Cluster (Stanford University). Gene clusters up-regulated in the S, G_2/M, and G_1 phases (*red*) were detected with cell-cycle progression. Canonical and noncanonical initiation factors and cell cycle–related genes are listed (*right*).

Functional Analysis of the Effect of HCV IRES–Related Canonical and Noncanonical Initiation Factors on Translation Directed by HCV IRES

To prove that the induction of the canonical and noncanonical initiation factors during S and G_2/M phases contributes to cell cycle–dependent translation of HCV, antisense phosphorothioate oligos were designed for La protein, PTB, eIF3 p170, eIF2γ, RNPL, PABPC-1, PCBP-2, and ribosomal protein S9, and HCV IRES activity was evaluated under the suppression of these factors. RT-PCR showed that expression of the targeted factors was significantly reduced by the antisense oligos, whereas that of β-actin did not significantly change (Figure 7*B*). Reduced expression of these factors was also evaluated by Western blotting (Figure 7*C*). The suppression of La protein, PTB, and eIF2γ specifically reduced HCV IRES activity to 40%, 50%, and 53% of the control level, respectively. The effect of inhibiting HCV IRES activity was equal to or greater than that exerted by an antisense oligo against 5′-NTR of HCV (nt 330–350). However, suppression of eIF3 p170, RNPL, PABPC-1, PCBP-2, and ribosomal protein S9 did not reduce HCV IRES activity (Figure 7*A*). To rule out the

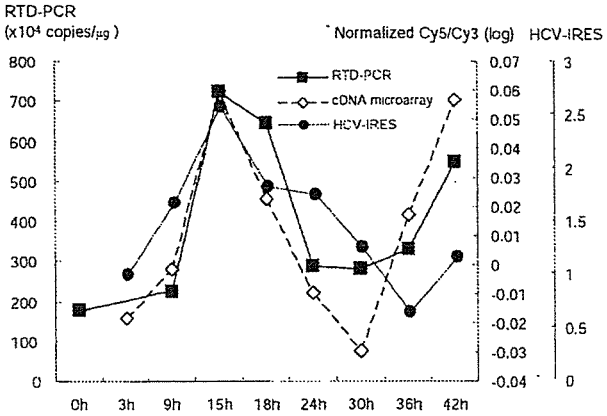

Figure 6. La protein expression in RCF-26 under cell-cycle progression determined by RTD-PCR. Normalized Cy5/Cy3 of mRNA expression of La protein and HCV IRES activities are shown in same dimension.

possibility that these reduced HCV IRES activities were not due to nonspecific suppression by the antisense oligos, antisense oligos to La protein, PTB, eIF3 p170, and ribosomal protein S9 were applied to ΔRCF-9 in which the functional HCV IRES element had been deleted. Two antisense oligos to La protein and PTB, which reduced HCV IRES activity in RCF-26, did not change HCV IRES activity in ΔRCF-9. Similarly, 2 antisense oligos to eIF3 p170 and ribosomal protein S9, which had no effect on HCV IRES activity, did not have any effect on HCV IRES activity in ΔRCF-9 (Figure 7*A*). Conversely, overexpression of La protein, PTB, and eIF3 p170 significantly enhanced HCV IRES activity in a dose-dependent manner, whereas the overexpression of eIF2γ, RNPL, PCBP-1, PCBP-2, and ribosomal protein S9 had no effect (Figure 8). The overexpression of La protein, PTB, and eIF3 p170 in ΔRCF-9 did not have any effect on HCV IRES activity (Figure 8). We also confirmed these findings in rabbit reticulocyte lysates by co-translating pRL-HL (HCV IRES reporter) and La protein, PTB, and eIF3 p170 (data not shown). Thus, of these HCV IRES–related canonical and noncanonical initiation factors, La protein and PTB significantly changed HCV IRES activity in both the suppressed and overexpressed states. Thus, changes in the expression of these factors alter HCV IRES activity in a cell cycle–dependent manner.

Expression of La Protein, Polypyrimidine Tract Binding Protein, and Eukaryotic Initiation Factor 3 in Lesions of Chronic Hepatitis C

To examine the functional role of these factors on HCV replication in the lesions of chronic hepatitis C, we evaluated their expression in 26 liver samples from patients with chronic hepatitis C and in 8 normal liver samples by RTD-PCR. Tables 3 and 4 list the clinical characteristics of the patients. The expression level of La protein in the specimens of the patients with chronic hepatitis C was significantly higher than that of the normal livers, whereas the expression of PTB and eIF3 p170 was not statistically different (Table 3). Some of these samples were also reevaluated by Northern blotting, and the results were similar (data not shown). Up-regulation of the La protein was related to neither the histological stage nor the activity of liver disease (Table 4). However, the expression of La protein was significantly correlated with the amount of HCV RNA in the liver (Figure 9). Moreover, HCV RNA replication was significantly higher in liver with high La protein expres-

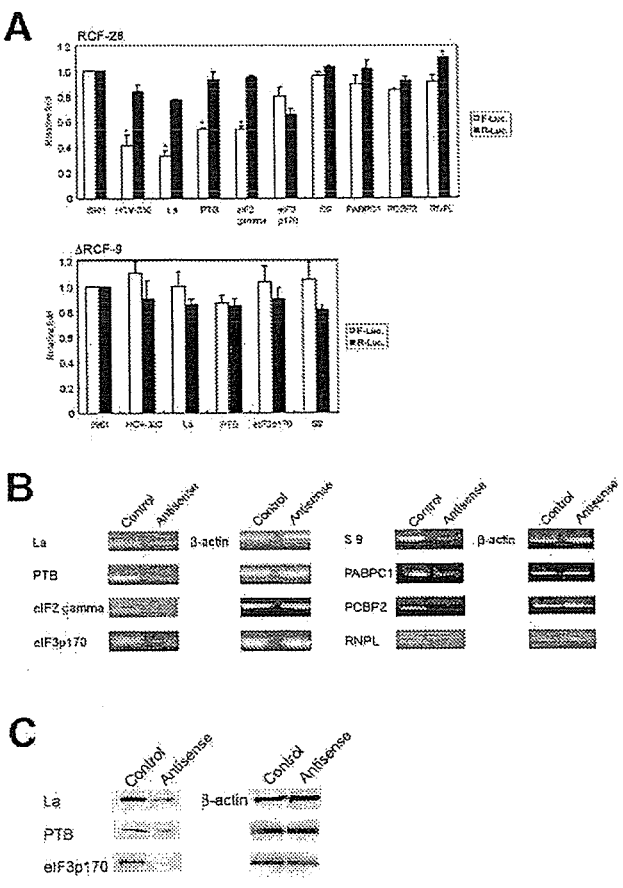

Figure 7. Suppression of HCV IRES–related canonical and noncanonical initiation factors (La protein, PTB, eIF3 [p170], eIF2γ, RNPL, PABPC-1, PCBP-2, and ribosomal protein S9) by specific antisense phosphorothioate oligos and HCV IRES activity in RCF-26 and ΔRCF-9. (*A*) Changes in *Renilla* (cap-dependent translation) and firefly luciferase (HCV IRES–directed translation) activities caused by suppression of these factors by antisense phosphorothioate oligos. $*P < .05$. (*B*) Suppression of factors confirmed by RT-PCR. (*C*) Suppression of factors confirmed by Western blotting.

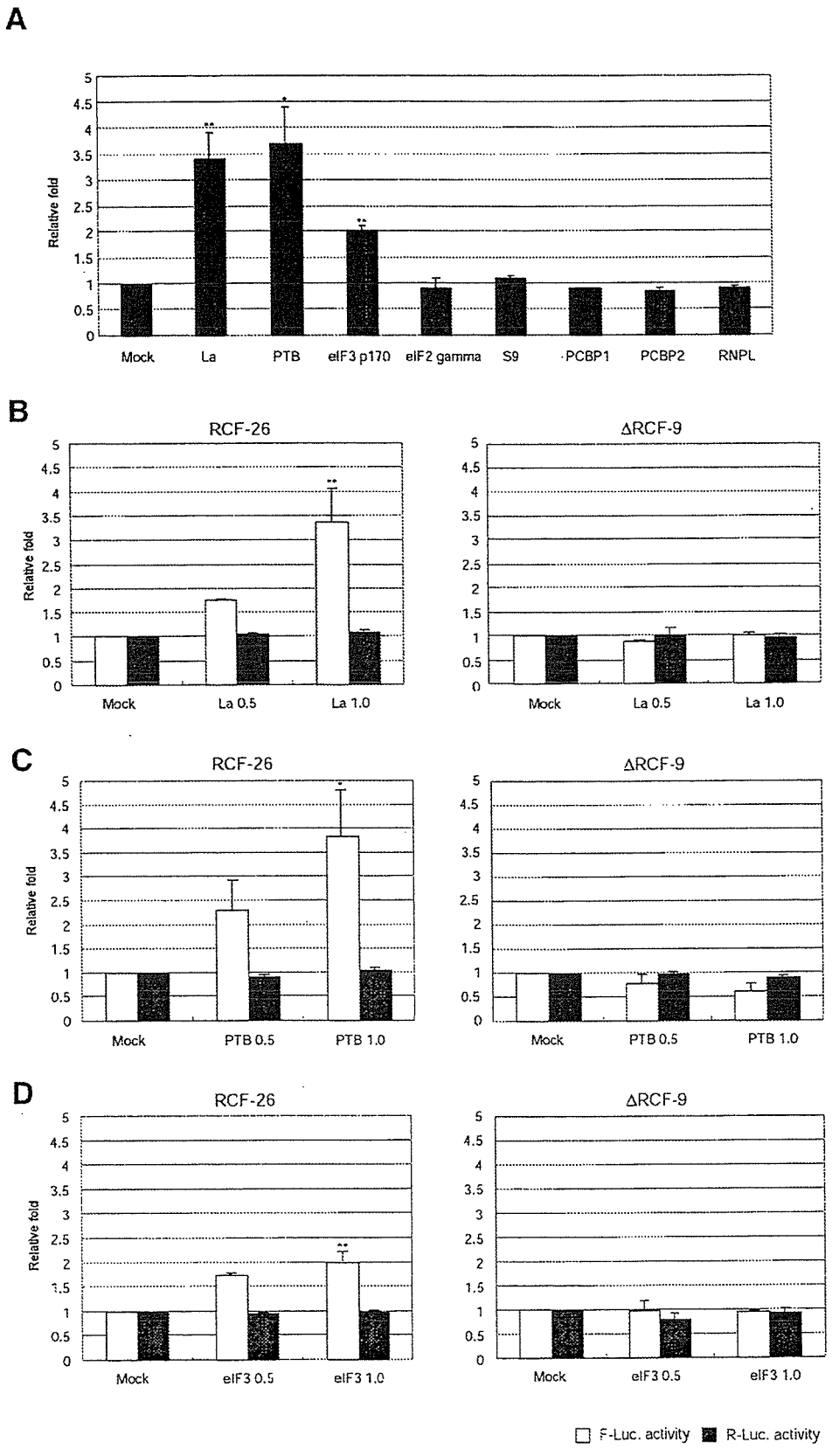

Figure 8. (*A*) Overexpression of HCV IRES–related canonical and noncanonical initiation factors (La protein, PTB, eIF3 [p170], eIF2γ, RNPL, PCBP-1, PCBP-2, and ribosomal protein S9) in RCF-26 and HCV IRES activity. (*B–D*) Dose-dependent overexpression of La protein, PTB, and eIF3 p170 in RCF-26 and ΔRCF-9. $*P < .05$; $**P < .01$.

Table 3. Expression of La Protein, PTB, and eIF3 (p170) in Liver Detected by RTD-PCR

Diagnosis	n	Age (y)	Sex (M:F)	ALT (*IU/L*)	Serological HCV type (group 1:group 2)	La (×10^6 *copies/μg*)	PTB-1 (×10^5 *copies/μg*)	eIF3 (p170) (×10^6 *copies/μg*)
Normal	8	64.5 ± 4.10	5:3	17.0 ± 9.86	ND	1.08 ± 0.11	1.34 ± 0.15	3.32 ± 0.46
Chronic hepatitis C	26	62.8 ± 2.27	20:6	67.7 ± 10.2[a]	21:3[b]	2.75 ± 0.26[c]	1.40 ± 0.14	2.21 ± 0.31

ALT, alanine aminotransferase; ND, not done.
[a]$P < .05$.
[b]Two patients were unclassified.
[c]$P < .01$.

sion (Figure 10). These findings indicate that La protein plays an important role in the replication of HCV in the livers of patients infected with chronic hepatitis C.

Discussion

Although extensive studies have examined the molecular biology of HCV, the responsible host factors that regulate HCV replication in patients with chronic hepatitis C have not yet been elucidated. Patients with a high viral load are refractory to interferon therapy, even when it is combined with ribavirin.[3–6] Recent advances in the HCV replicon system have shown some adaptive mutations in the HCV genome (NS5A or NS3) for efficient replication of cellular factors that inhibit HCV replication, such as PKR and interferon-regulatory protein 1.[40] However, there has been no clear evidence that these factors are truly determinant of HCV replication in patients with chronic hepatitis C. The identification of host factors that regulate HCV replication in vivo should show the underlying mechanism of high viral load in patients with chronic hepatitis C. Moreover, it could provide a basis for the development of a new antiviral treatment strategy.

The translation of viral polyprotein is an important step in viral replication and could thus present a target for a novel antiviral therapy. Translation of the HCV RNA genome is initiated by a highly structured RNA segment, the IRES, that occupies most of the 5′-NTR RNA.[7–15] We showed that HCV IRES activity varies during different phases of the cell cycle: it is highest during the S and M phases and lowest during the G_0 phase of the cell cycle.[22] These findings have important clinical relevance because viral translation might be enhanced by factors that stimulate the regeneration of hepatocytes in patients with chronic hepatitis C. We investigated the molecular basis of these findings and found host factors that regulate HCV IRES.

The expression of La protein, PTB, eIF3, and eIF2γ was repressed in confluent and serum-starved cells, but eIF3 and eIF2γ were reduced in confluent or serum-starved cells. Analysis of cell-cycle progression more precisely showed the interaction of these initiation factors with the cell cycle–dependent regulation of HCV IRES activity. Most of the HCV IRES–related canonical and noncanonical initiation factors (PCBP-2, PTB, eIF3, eIF2γ, eIF2β, La protein, and RNLPL) were induced during the S and G_2/M phases of the cell cycle. Conversely, eIF4A, eIF4B, and PABPC-1, which are not supposed to be a requirement for HCV IRES activity,[33,39] were induced during G_1. In cells, because protein translation takes place immediately in the presence of mRNA, dynamism of expression profiles might directly link to HCV IRES activity, although some protein levels were also regulated by the posttranslational modification. The finding that HCV uses host factors induced during cell division (S and G_2/M), but not during quiescence (G_0/G_1), is of interest. In this respect, HCV IRES–directed translation differed from either cap-dependent or IRES-directed translation by encephalomyocarditis virus and the picornavirus-like group. Reports indicate that eIF4B and PABPC-1 are required for encephalomyocarditis virus and poliovirus, but not for HCV translation.[39] G_1 induction of the ribosomal protein S9, which supposedly binds the secondary structure of HCV IRES,[7] seems controversial. To further investigate these findings, we evaluated the functional roles of these factors in HCV IRES activity. Among the canonical and noncanonical HCV IRES–related initiation factors, the suppression of PTB, La protein, and eIF2γ by using antisense oligos reduced HCV IRES activity, and the overexpression of PTB, La, and eIF3 stimulated HCV IRES activity. The La protein and PTB changed HCV IRES activity in both

Table 4. Histological Findings and La Protein Expression

Histology	n	La (×10^6 *copies/μg*)
F1	2	1.98 ± 0.03
F2	6	3.31 ± 0.80
F3	7	3.04 ± 0.48
F4	11	2.40 ± 0.30
A1	10	2.72 ± 0.52
A2	15	2.82 ± 0.30
A3	1	1.86

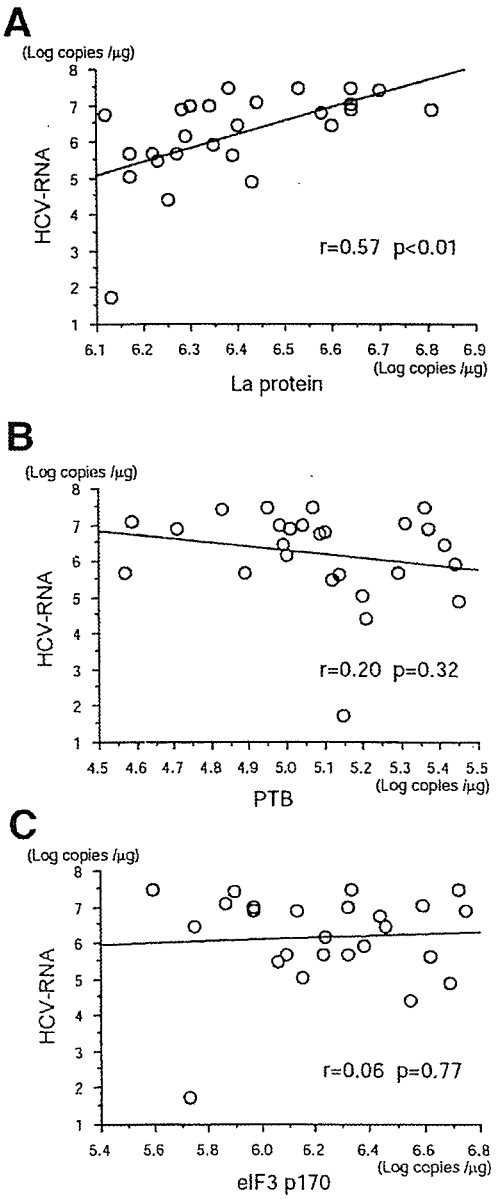

Figure 9. Correlation of La protein (*A*), PTB (*B*), and eIF3 p170 (*C*) with the amount of HCV RNA in tissue lesions of chronic hepatitis C.

the suppressed and overexpressed states. However, neither suppression nor overexpression of ribosomal protein S9 affected HCV IRES activity. Thus, this study could not identify the functional significance of ribosomal protein S9 for HCV IRES activity.

The definition of these initiation factors has very important clinical relevance to HCV replication. We therefore investigated the expression of La protein, PTB, and eIF3 in tissue lesions from patients with chronic hepatitis C. Expression of La protein was significantly increased in the liver of patients, whereas that of PTB and eIF3 did not significantly increase. Neither histological activity nor stage was associated, but the amount of liver HCV RNA was significantly correlated with the level of La protein expression. Patients that expressed high levels of La protein in the liver were infected with more HCV (Figure 10). Thus, La protein plays an important role in HCV replication in livers of patients with chronic hepatitis C. Two possible mechanisms might explain the induction of La protein in the livers of chronic hepatitis C patients. First, significant proportions of cells undergo division during hepatocyte regeneration, and the proportion of cells in M phase that lead to the induction of the La protein increases. Second, HCV induces La protein. Because the expression of PTB and eIF3 was not significantly induced in the tissue lesions of chronic hepatitis C patients in this study, there must be unknown mechanisms by which HCV infection induces La protein. Our preliminary results showed that HCV proteins increased La protein in Huh-7 cells (data not shown). Further analysis is needed to show the interaction between La protein induction and HCV replication in chronic hepatitis C.

In conclusion, we discovered host factors that regulate HCV translation and replication in the liver. The implication of these findings with regard to the HCV life cycle is shown in Figure 11. Hepatitis and the resulting increased regeneration of hepatocytes increase IRES activity and enhance HCV replication. This may be an important mechanism by which HCV maintains its viral load under host defense immune pressure. These findings shed new light on the mechanism of HCV replication and could be the basis for developing a novel antiviral therapy. Although La protein and PTB have been shown to be involved in the cell-cycle regulation of HCV IRES activity, many other host factors might also be involved.

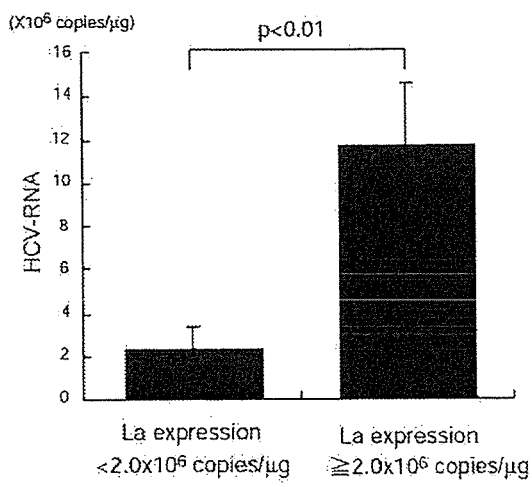

Figure 10. La protein expression and HCV RNA in liver.

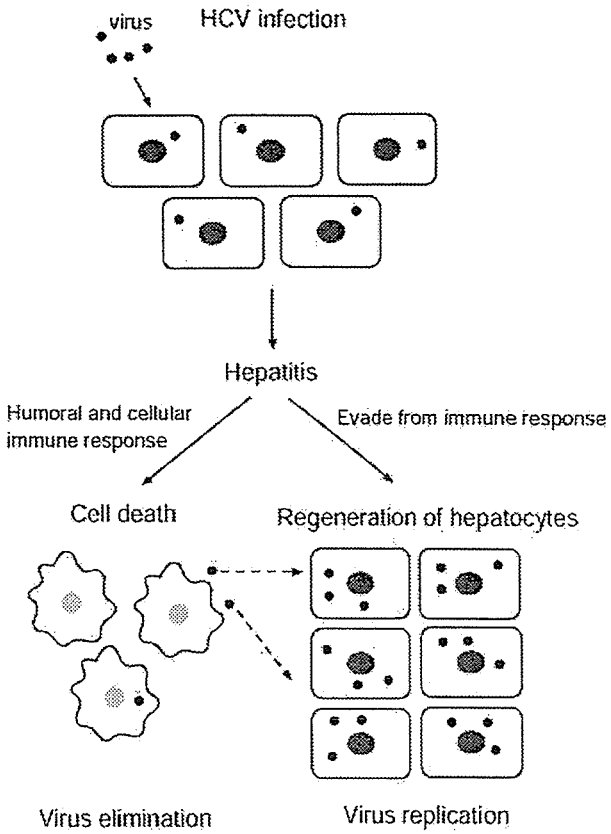

Figure 11. Hepatitis and HCV life cycle.

We are extending these analyses to other initiation factors and investigating the functional role on HCV IRES activity and replication of HCV.

References

1. Choo QL, Kuo G, Weiner AJ, Overby LR, Bradley DW, Houghton M. Isolation of a cDNA clone derived from a blood-borne non-A, non-B viral hepatitis genome. Science 1989;244:359–362.
2. Kiyosawa K, Sodeyama T, Tanaka E, Gibo Y, Yoshizawa K, Nakano Y, Furuta S, Akahane Y, Nishioka K, Purcell RH, et al. Interrelationship of blood transfusion, non-A, non-B hepatitis and hepatocellular carcinoma: analysis by detection of antibody to hepatitis C virus. Hepatology 1990;12:671–675.
3. Davies MV, Pelletier J, Meerovitch K, Sonenberg N, Kaufman RJ. The effect of poliovirus proteinase 2Apro expression on cellular metabolism. Inhibition of DNA replication, RNA polymerase II transcription, and translation. J Biol Chem 1991;266: 14714–14720.
4. McHutchison JG, Gordon SC, Schiff ER, Shiffman ML, Lee WM, Rustgi VK, Goodman ZD, Ling MH, Cort S, Albrecht JK. Interferon alfa-2b alone or in combination with ribavirin as initial treatment for chronic hepatitis C. Hepatitis Interventional Therapy Group. N Engl J Med 1998;339:1485–1492.
5. Poynard T, Marcellin P, Lee SS, Niederau C, Minuk GS, Ideo G, Bain V, Heathcote J, Zeuzem S, Trepo C, Albrecht J. Randomised trial of interferon alpha2b plus ribavirin for 48 weeks or for 24 weeks versus interferon alpha2b plus placebo for 48 weeks for treatment of chronic infection with hepatitis C virus. International Hepatitis Interventional Therapy Group (IHIT). Lancet 1998;352:1426–1432.
6. Fried MW, Shiffman ML, Reddy KR, Smith C, Marinos G, Goncales FL Jr, Haussinger D, Diago M, Carosi G, Dhumeaux D, Craxi A, Lin A, Hoffman J, Yu J. Peginterferon alfa-2a plus ribavirin for chronic hepatitis C virus infection. N Engl J Med 2002;347:975–982.
7. Pestova TV, Shatsky IN, Fletcher SP, Jackson RJ, Hellen CU. A prokaryotic-like mode of cytoplasmic eukaryotic ribosome binding to the initiation codon during internal translation initiation of hepatitis C and classical swine fever virus RNAs. Genes Dev 1998;12:67–83.
8. Wang C, Sarnow P, Siddiqui A. Translation of human hepatitis C virus RNA in cultured cells is mediated by an internal ribosome-binding mechanism. J Virol 1993;67:3338–3344.
9. Reynolds JE, Kaminski A, Kettinen HJ, Grace K, Clarke BE, Carroll AR, Rowlands DJ, Jackson RJ. Unique features of internal initiation of hepatitis C virus RNA translation. EMBO J 1995;14:6010–6020.
10. Lu HH, Wimmer E. Poliovirus chimeras replicating under the translational control of genetic elements of hepatitis C virus reveal unusual properties of the internal ribosomal entry site of hepatitis C virus. Proc Natl Acad Sci U S A 1996;93:1412–1417.
11. Honda M, Ping LH, Rijnbrand RC, Amphlett E, Clarke B, Rowlands D, Lemon SM. Structural requirements for initiation of translation by internal ribosome entry within genome-length hepatitis C virus RNA. Virology 1996;222:31–42.
12. Wang C, Sarnow P, Siddiqui A. A conserved helical element is essential for internal initiation of translation of hepatitis C virus RNA. J Virol 1994;68:7301–7307.
13. Rijnbrand RC, Abbink TE, Haasnoot PC, Spaan WJ, Bredenbeek PJ. The influence of AUG codons in the hepatitis C virus 5′ nontranslated region on translation and mapping of the translation initiation window. Virology 1996;226:47–56.
14. Honda M, Brown EA, Lemon SM. Stability of a stem-loop involving the initiator AUG controls the efficiency of internal initiation of translation on hepatitis C virus RNA. RNA 1996;2:955–968.
15. Honda M, Beard MR, Ping LH, Lemon SM. A phylogenetically conserved stem-loop structure at the 5′ border of the internal ribosome entry site of hepatitis C virus is required for cap-independent viral translation. J Virol 1999;73:1165–1174.
16. Ali N, Siddiqui A. The La antigen binds 5′ noncoding region of the hepatitis C virus RNA in the context of the initiator AUG codon and stimulates internal ribosome entry site-mediated translation. Proc Natl Acad Sci U S A 1997;94:2249–2254.
17. Ali N, Pruijn GJ, Kenan DJ, Keene JD, Siddiqui A. Human La antigen is required for the hepatitis C virus internal ribosome entry site-mediated translation. J Biol Chem 2000;275:27531–27540.
18. Ali N, Siddiqui A. Interaction of polypyrimidine tract-binding protein with the 5′ noncoding region of the hepatitis C virus RNA genome and its functional requirement in internal initiation of translation. J Virol 1995;69:6367–6375.
19. Chung RT, Kaplan LM. Heterogeneous nuclear ribonucleoprotein I (hnRNP-I/PTB) selectively binds the conserved 3′ terminus of hepatitis C viral RNA. Biochem Biophys Res Commun 1999;254: 351–362.
20. Spangberg K, Schwartz S. Poly(C)-binding protein interacts with the hepatitis C virus 5′ untranslated region. J Gen Virol 1999; 80:1371–1376.
21. Sachs AB. Cell cycle-dependent translation initiation: IRES elements prevail. Cell 2000;101:243–245.
22. Honda M, Kaneko S, Matsushita E, Kobayashi K, Abell GA, Lemon SM. Cell cycle regulation of hepatitis C virus internal ribosomal entry site-directed translation. Gastroenterology 2000; 118:152–162.
23. Shimazaki T, Honda M, Kaneko S, Kobayashi K. Inhibition of internal ribosomal entry site-directed translation of HCV by re-

combinant IFN-alpha correlates with a reduced La protein. Hepatology 2002;35:199–208.
24. Gosert R, Chang KH, Rijnbrand R, Yi M, Sangar DV, Lemon SM. Transient expression of cellular polypyrimidine-tract binding protein stimulates cap-independent translation directed by both picornaviral and flaviviral internal ribosome entry sites in vivo. Mol Cell Biol 2000;20:1583–1595.
25. Siomi MC, Eder PS, Kataoka N, Wan L, Liu Q, Dreyfuss G. Transportin-mediated nuclear import of heterogeneous nuclear RNP proteins. J Cell Biol 1997;138:1181–1192.
26. Wang X, Liebhaber SA. Complementary change in cis determinants and trans factors in the evolution of an mRNP stability complex. EMBO J 1996;15:5040–5051.
27. Gaspar NJ, Kinzy TG, Scherer BJ, Humbelin M, Hershey JW, Merrick WC. Translation initiation factor eIF-2. Cloning and expression of the human cDNA encoding the gamma-subunit. J Biol Chem 1994;269:3415–3422.
28. Johnson KR, Merrick WC, Zoll WL, Zhu Y. Identification of cDNA clones for the large subunit of eukaryotic translation initiation factor 3. Comparison of homologues from human, *Nicotiana tabacum*, *Caenorhabditis elegans*, and *Saccharomyces cerevisiae*. J Biol Chem 1997;272:7106–7113.
29. Hanecak R, Brown-Driver V, Fox MC, Azad RF, Furusako S, Nozaki C, Ford C, Sasmor H, Anderson KP. Antisense oligonucleotide inhibition of hepatitis C virus gene expression in transformed hepatocytes. J Virol 1996;70:5203–5212.
30. Honda M, Kaneko S, Kawai H, Shirota Y, Kobayashi K. Differential gene expression between chronic hepatitis B and C hepatic lesion. Gastroenterology 2001;120:955–966.
31. Kruger M, Beger C, Li QX, Welch PJ, Tritz R, Leavitt M, Barber JR, Wong-Staal F. Identification of eIF2Bgamma and eIF2gamma as cofactors of hepatitis C virus internal ribosome entry site-mediated translation using a functional genomics approach. Proc Natl Acad Sci U S A 2000;97:8566–8571.
32. Buratti E, Tisminetzky S, Zotti M, Baralle FE. Functional analysis of the interaction between HCV 5'UTR and putative subunits of eukaryotic translation initiation factor eIF3. Nucleic Acids Res 1998;26:3179–3187.
33. Michel YM, Borman AM, Paulous S, Kean KM. Eukaryotic initiation factor 4G-poly(A) binding protein interaction is required for poly(A) tail-mediated stimulation of picornavirus internal ribosome entry segment-driven translation but not for-X-mediated stimulation of hepatitis C virus translation. Mol Cell Biol 2001;21:4097–4109.
34. Cornelis S, Bruynooghe Y, Denecker G, Van Huffel S, Tinton S, Beyaert R. Identification and characterization of a novel cell cycle-regulated internal ribosome entry site. Mol Cell 2000;5:597–605.
35. Sachs AB, Sarnow P, Hentze MW. Starting at the beginning, middle, and end: translation initiation in eukaryotes. Cell 1997;89:831–838.
36. Kawai HF, Kaneko S, Honda M, Shirota Y, Kobayashi K. Alpha-fetoprotein-producing hepatoma cell lines share common expression profiles of genes in various categories demonstrated by cDNA microarray analysis. Hepatology 2001;33:676–691.
37. Shirota Y, Kaneko S, Honda M, Kawai HF, Kobayashi K. Identification of differentially expressed genes in hepatocellular carcinoma with cDNA microarrays. Hepatology 2001;33:832–840.
38. Takeuchi T, Katsume A, Tanaka T, Abe A, Inoue K, Tsukiyama-Kohara K, Kawaguchi R, Tanaka S, Kohara M. Real-time detection system for quantification of hepatitis C virus genome. Gastroenterology 1999;116:636–642.
39. Pestova TV, Kolupaeva VG, Lomakin IB, Pilipenko EV, Shatsky IN, Agol VI, Hellen CU. Molecular mechanisms of translation initiation in eukaryotes. Proc Natl Acad Sci U S A 2001;98:7029–7036.
40. Pflugheber J, Fredericksen B, Sumpter R Jr, Wang C, Ware F, Sodora DL, Gale M Jr. Regulation of PKR and IRF-1 during hepatitis C virus RNA replication. Proc Natl Acad Sci U S A 2002;99:7029–7036.

Received March 16, 2004. Accepted November 4, 2004.

Address requests for reprints to: Shuichi Kaneko, MD, PhD, Department of Gastroenterology, Graduate School of Medicine, Kanazawa University, Takara-Machi 13-1, Kanazawa, 920-8641, Japan. e-mail: skaneko@medf.m.kanazawa-u.ac.jp; fax: (81) 76-234-4250.

The authors thank Masami Ueda, Junko Hara, and Mikiko Nakamura for excellent technical assistance.

Int. J. Cancer: 118, 1194–1204 (2006)

Identification of α-fetoprotein-derived peptides recognized by cytotoxic T lymphocytes in HLA-A24+ patients with hepatocellular carcinoma

Eishiro Mizukoshi, Yasunari Nakamoto, Hirokazu Tsuji, Tatsuya Yamashita and Shuichi Kaneko*

Department of Gastroenterology, Graduate School of Medicine, Kanazawa University, Kanazawa, Ishikawa, Japan

α-Fetoprotein (AFP) has been proposed as a potential target for T-cell-based immunotherapy for hepatocellular carcinoma (HCC), but the number of its epitopes that have been identified is limited and the status of AFP-specific immunological responses in HCC patients has not been well-characterized. To address the issue, we examined the possibility of inducing AFP-specific cytotoxic T cells (CTLs) using novel HLA-A*2402-restricted T-cell epitopes (HLA, human leukocyte antigen) derived from AFP and then analyzed the relationship between its frequency of occurrence and clinical features associated with patients having HCC. Five AFP-derived peptides containing HLA-A*2402 binding motifs and showing high binding affinity to HLA-A*2402 induced CTLs to produce IFN-γ and kill an AFP-producing hepatoma cell line. The frequency of AFP-specific CTLs was 30–190 per 1 × 10^6 peripheral blood mononuclear cells, which was the same as that of other immunogenic cancer associated antigen-derived epitopes. Analyses of the relationships between AFP-specific CTL responses and clinical features of patients with HCC revealed that AFP epitopes were more frequently recognized by CTLs in patients with advanced HCC correlating to tumor factors or the stage of TNM classification. The analyses of CTL responses before and after HCC treatments showed that the treatments changed the frequency of AFP-specific CTLs. In conclusion, we identified five HLA-A*2402-restricted T-cell epitopes derived from AFP. The newly identified AFP epitopes could be a valuable component of HCC immunotherapy and for analyzing host immune responses to HCC.

Key words: immune response; epitope; CD8; HLA-A24; hepatitis

Introduction

Hepatocellular carcinoma (HCC) is a malignancy[1,2] and has gained major clinical interest because of its increasing incidence.[3] Several current advances in therapeutic modalities such as surgical hepatic resection, percutaneous tumor ablation by ethanol injection or radiofrequency (RF), transcatheter arterial embolization (TAE), chemotherapy and liver transplantation have improved the prognosis of HCC patients.[4–9] However, the survival of those who have advanced HCC is still not satisfactory, since most of these patients have numerous tumors or vascular invasions, which conventional therapeutic modalities cannot eradicate completely and therefore keep recurring. Therefore, the development of new antitumor therapies for advanced HCC patients remains an urgent and important field of research.

To eradicate HCC and to protect the patients from its recurrence, tumor antigen-specific immunotherapy is an attractive strategy like the immunotherapy of melanoma and other cancers.[10,11] Tumor-specific immune responses are mediated by $CD4^+$ and $CD8^+$ T-cell responses. $CD8^+$ T cells mediate antigen-specific and major histocompatibility complex (MHC)-restricted cytotoxic effects by recognition of peptides presented by MHC class I molecules through their TCR complex. Although many tumor-specific antigens have been identified in various cancers, the number of HCC-specific antigens known is still limited.

α-Fetoprotein (AFP) is a nonmutated oncofetal protein with tumor-selective expression that is frequently expressed in HCC, and its measurement in the serum is important for the diagnosis and monitoring of responses to treatment.[12] On the other hand, AFP expression in the normal liver is low or not detectable. Therefore, AFP is a target of interest for immunotherapy.

Recently, several results regarding AFP-specific cytotoxic T-cell responses were reported for human and mice studies.[13–16] These reports revealed that AFP-specific cytotoxic T cells (CTLs) induced by stimulation with peptides or DNA-based immunization kill AFP-producing hepatoma cell lines, suggesting that AFP-reactive T-cell clones are not deleted from the human T-cell repertoire and that AFP may be a useful tumor-specific antigen as a target for T-cell-based immunotherapy against HCC. However, the number of AFP epitopes that have been identified is limited and the status of AFP-specific immunological responses has not been well-characterized in patients with HCC.

In the current study, using novel HLA-A*2402-restricted T-cell epitopes (HLA, human leukocyte antigen) derived from AFP, we found that AFP-specific T-cell responses exist in patients with HCC but are weak during the early stage of the tumor, and that anticancer treatment can enhance host immune responses. By studying peripheral blood mononuclear cells (PBMCs) from 38 patients, we have shown that the induction of AFP-specific T cells is possible independent of hepatitis viral infection and that the number of AFP-specific T cells is as frequent as that of other tumor associated antigens in patients with advanced HCC. Moreover, HCC treatment dramatically changes the strength of AFP-specific immune responses, mostly by increasing the frequency of AFP-specific $CD8^+$ T-cell responses. These results provide a rationale for T-cell-based immunotherapy for HCC and suggest that the identified AFP epitopes could be a valuable component of HCC therapy and for analyzing host immune responses to HCC.

Material and methods

Patient population

In our study, we examined 38 HLA-A24 positive patients with HCC who were admitted to Kanazawa University Hospital between January 2002 and August 2003, consisting of 30 men and 8 women ranging from 46 to 80 years, with a mean age of 68.6 ± 7.0. HCCs were detected by imaging modalities such as dynamic CT scan, MR imaging, and abdominal arteriography. The diagnosis of HCC was histologically confirmed by taking US-guided needle biopsy specimens from 17 patients, surgical resection from 3 patients and autopsy from 4 patients. For the remaining 14 patients, diagnosis was made by typical hypervascular tumor staining on angiography in addition to using typical findings, which showed hyperattenuation areas in the early phase and hypoattenuation in the late phase on dynamic CT.[17] All subjects were negative for Abs to human immunodeficiency virus (HIV) and gave informed consent to this study in accordance with the Helsinki declaration. Eleven healthy blood donors with HLA-A24, who did not have a history of cancer and were negative for HBsAg and anti-hepatitis C virus antibody (HCVAb) served as controls.

Treatment of HCC

After diagnosis, 12 patients were treated by percutaneous tumor ablation using percutaneous ethanol injection therapy or RF ablation, 3 by TAE, 4 by chemotherapy, 3 by surgical operation, 13 by

*Correspondence to: Department of Gastroenterology, Graduate School of Medicine, Kanazawa University, Kanazawa, Ishikawa 920-8641, Japan. Fax: +81-76-234-4250. E-mail: skaneko@medf.m.kanazawa-u.ac.jp
Received 28 February 2005; Accepted after revision 5 July 2005
DOI 10.1002/ijc.21468
Published online 8 September 2005 in Wiley InterScience (www.interscience.wiley.com).

TABLE I – CHARACTERISTICS OF THE PATIENTS STUDIED

Case	Age (years)	Sex (M/F)	AFP level (ng/ml)	Diff. degree[1]	Tumor size[2]	Tumor multiplicity	Vascular invasion	TNM stage[3]	Nontumor liver	Liver function	Etiology[4]	Treatment
1	67	M	46	Mod	Large	Multiple	–	II	Cirrhosis	Child A	HCV	TAE + RF
2	72	M	16	Wel	Large	Multiple	–	II	Cirrhosis	Child A	HCV	RF
3	69	M	22	ND	Small	Multiple	–	II	Cirrhosis	Child B	HCV	RF
4	58	F	50,800	ND	Large	Multiple	+	IIIc	Cirrhosis	Child B	HCV	Chemotherapy
5	65	F	94	ND	Small	Solitary	–	I	Cirrhosis	Child C	HCV	No treatment
6	72	M	12	ND	Small	Solitary	–	I	Cirrhosis	Child B	HCV	RF
7	66	M	471	ND	Large	Multiple	+	IV	Cirrhosis	Child A	HCV	TAE + RF
8	79	M	19	Mod	Large	Multiple	+	IIIc	Cirrhosis	Child A	HCV	TAE + PETT
9	63	M	154	Mod	Large	Solitary	–	I	Chronic hepatitis	Child A	HBV	Surgical resection
10	70	F	13	Wel	Large	Solitary	–	I	Cirrhosis	Child A	HCV	RF
11	67	M	41	Wel	Large	Multiple	–	IV	Cirrhosis	Child B	HCV	TAE + chemotherapy
12	67	F	330	Wel	Small	Solitary	–	I	Cirrhosis	Child A	HCV	TAE + RF
13	69	M	13	ND	Large	Solitary	–	I	Cirrhosis	Child A	HCV	TAE
14	73	M	332	Mod	Large	Solitary	+	IV	Cirrhosis	Child B	HCV	TAE + chemotherapy
15	56	M	<10	ND	Large	Multiple	+	IV	Chronic hepatitis	Child A	HBV	Chemotherapy
16	66	F	<10	ND	Large	Multiple	+	IIIa	Cirrhosis	Child A	HCV	Chemotherapy
17	55	M	<10	ND	Small	Solitary	–	I	Cirrhosis	Child B	HCV	RF
18	77	M	75	Wel	Small	Multiple	+	IIIa	Cirrhosis	Child A	HCV	TAE + RF
19	54	M	21	Mod	Large	Multiple	–	II	Cirrhosis	Child A	HCV	RF
20	71	M	<10	Mod	Large	Multiple	–	II	Cirrhosis	Child A	NBNC	RF
21	80	M	94	ND	Large	Multiple	–	II	Cirrhosis	Child A	HCV	TAE + PEIT
22	73	M	26	Mod	Large	Multiple	+	IIIb	Cirrhosis	Child A	HCV	Chemotherapy
23	59	M	1260	Wel	Large	Multiple	+	II	Cirrhosis	Child B	HCV	TAE + RF
24	59	M	<10	ND	Large	Solitary	–	IIIa	Cirrhosis	Child A	HBV	TAE + RF
25	46	M	287	Mod	Small	Solitary	–	I	Cirrhosis	Child A	HCV	Surgical resection
26	68	M	46	Wel	Small	Multiple	–	II	Cirrhosis	Child A	HCV	PEIT
27	52	M	11,291	Por	Large	Multiple	+	IIIa	Chronic hepatitis	Child C	HBV	TAE + RF
28	66	F	67	Mod	Large	Multiple	–	II	Cirrhosis	Child B	HCV	TAE
29	66	F	247	ND	Large	Multiple	+	IIIa	Cirrhosis	Child A	HCV	TAE
30	76	M	16	ND	Small	Solitary	–	I	Cirrhosis	Child A	HCV	RF
31	62	M	341	Mod	Large	Multiple	–	II	Cirrhosis	Child B	HCV	TAE + RF
32	71	M	<10	Wel	Large	Multiple	–	II	Chronic hepatitis	Child A	HCV	TAE + RF
33	76	M	<10	Wel	Large	Solitary	–	I	Chronic hepatitis	Child A	HCV	Surgical resection
34	79	M	22	Wel	Large	Multiple	–	II	Cirrhosis	Child B	HCV	TAE + RF
35	67	M	18	Wel	Large	Solitary	–	I	Cirrhosis	Child A	HCV	PEIT
36	70	F	30	Mod	Small	Solitary	–	I	Cirrhosis	Child B	HCV	RF
37	71	M	<10	Mod	Large	Multiple	–	II	Cirrhosis	Child A	HCV	RF
38	58	M	46	ND	Large	Solitary	–	I	Cirrhosis	Child B	NBNC	TAE + RF

wel, well differentiated; mod, moderately differentiated; por, poorly differentiated; ND, not determined.
[1]Histological degree of HCC.–[2]Tumor size was divided into either 'small' (≦ 2 cm) or 'large' (>2 cm).–[3]TNM stage according to the Union Internationale Contre Le Cancer (UICC) classification system (6th version).–[4]NBNC, nonB, nonC.

a combination of TAE and perucutaneous tumor ablation and 2 by a combination of TAE and chemotherapy. The characteristics of the patients are shown in Table I. The treatment efficacy was evaluated by complete necrosis of the tumor lesion using dynamic CT after the completion of the treatment. Follow-ups were conducted at outpatient clinics, using blood tests, USG and dynamic CT, every 3 months for 1 year. Blood samples, including lymphocytes, were drawn from patients before and 1–3 months after treatment.

Laboratory and virologic testing

Blood samples were tested for HBsAg, HCVAb and HIVAb by commercial immunoassays (Fuji Rebio, Tokyo, Japan). Epstein-Barr virus (EBV) and cytomegalo virus (CMV) serology was done by standard enzyme immunoassay (EIA) techniques for the detection of the specific IgG, using commercial assays. HLA typing of PBMC from patients and normal donors was performed by complement-dependent microcytotoxicity, using HLA typing trays purchased from One Lambda (Canoga Park, CA).

Serum AFP level was measured by EIA (AxSYM AFP, Abbott Japan, Tokyo, Japan) and pathological grading of tumor cell differentiation was assessed according to the general rules for the clinical and pathologic study of primary liver cancer.[18] The severity of liver disease (stage of fibrosis) was evaluated according to the criteria of Desmet et al.[19] using the biopsy specimens of liver tissue, where F4 was defined as cirrhosis.

Synthetic peptides

To identify potential HLA-A24-binding peptides within AFP (GenBank accession number J00077, J00076 and V01514), a computer-based program available at BioInformatics and Molecular Analysis Section (BIMAS) website was employed. The HLA-A24 restricted epitopes derived from HIV envelope protein,[20] EBV latent membrane protein 2A[21] and CMV pp65[22] were used as control peptides to test for T-cell responses, and the HLA-A2 restricted epitope derived from AFP[14] was used as a control peptide for HLA-A24 stabilization assay. Peptides were synthesized at Mimotope (Melbourne, Australia) and Sumitomo Pharmaceuticals (Osaka, Japan). They were identified using mass spectrometry, and their purities were determined to be >80% by analytical HPLC.

Cell lines

Three human hepatoma cell lines, HepG2, Huh7 and HLE, were cultured in DMEM (Gibco, Grand Island, NY) with 10% fetal calf serum (FCS) (Gibco).

T2-A24 cells, which were transfected with HLA-A*2402 molecule into T2 cells,[22] were cultured in RPMI 1640 medium contain-

TABLE II – PEPTIDES

Peptide	Source	Start position	Amino acid sequence	HLA restriction	Score[1]
AFP_{403}	AFP	403	KYIQESQAL	HLA-A24	720
AFP_{424}	AFP	424	EYYLQNAFL	HLA-A24	200
AFP_{434}	AFP	434	AYTKKAPQL	HLA-A24	200
AFP_{357}	AFP	357	EYSRRHPQL	HLA-A24	200
AFP_{150}	AFP	150	AYEEDRETF	HLA-A24	180
AFP_{504}	AFP	504	SYANRRPCF	HLA-A24	100
AFP_{591}	AFP	591	CFAEEGQKL	HLA-A24	32
AFP_{414}	AFP	414	RSCGLFQKL	HLA-A24	15
AFP_{7}	AFP	7	IFLIFLLNF	HLA-A24	15
AFP_{322}	AFP	322	KPEGLSPNL	HLA-A24	14
$HIVenv_{584}$	HIV envelope	584	RYLRDQQLL	HLA-A24	720
$EBV1m_{287}$	EBV latent membarne	287	TYGPVFMSL	HLA-A24	403
$CMVpp65_{328}$	CMV pp65	328	QYDPVAALF	HLA-A24	120
AFP_{137}	AFP	137	PLFQVPEPV	HLA-A2	3

[1]Estimated half-time of dissociation from the HLA-A24 allele (min).

ing 10% FCS and 800 μg/ml G418 (GibcoBRL, Grand Island, NY). The HLA-A*2402 gene-transfected C1R cell line (C1R-A24)[23] was cultured in RPMI 1640 medium containing 10% FCS and 500 μg/ml hygromycin B (Sigma, St Louis, MO), and K562 was cultured in RPMI 1640 medium containing 10% FCS. All medium contained 100 U/ml penicillin and 100 μg/ml streptomycin (GibcoBRL).

Preparation of PBMCs

Blood samples were diluted twice in phosphate-buffered saline (PBS) and loaded on ficoll gradients (AXIS-SHIELD PoC AS, Oslo, Norway) in 50 ml tubes. After centrifugation at 900*g* for 22 min at room temperature, PBMCs were harvested from the interphase, resuspended in PBS and centrifuged again at 600*g*. Each cell pellet was resuspended in PBS, centrifuged at 300*g* for 8 min and finally resuspended in complete culture medium consisting of RPMI, 10% heat inactivated FCS, 100 U/ml penicillin and 100 μg/ml streptomycin. Fresh PBMCs were used for CTL assay, and the remaining PBMC were resuspended in RPMI 1640 containing 80% FCS and 10% dimethyl sulfoxide (Sigma) and cryopreserved until use.

MHC binding assay

Peptide binding assays were performed as previously described,[24] with the following modification. T2-A24 cells (transporter associated with antigen processing [TAP]-deficient human lymphoid-derived cells transfected with HLA-A*2402 molecule) were cultured for 16 hr at 26°C to enhance the expression of peptide-receptive cell surface molecules. After the addition of synthetic peptides, the cells were incubated at 37°C for 2 hr to unfold HLA-A*2402 molecules not stabilized by peptide binding. The cells were then washed and stained with anti-HLA-A24 monoclonal antibody (Sankojunyaku, Tokyo, Japan), anti-mouse immunoglobulin conjugated FITC (DAKO, Glostrup, Denmark) and 1 μg/ml of propidium iodide. Live cells were gated based on forward and side scattering and the exclusion of propidium iodide-positive cells. The data were expressed as the mean fluorescence intensity (MFI) or % MFI increase, which was calculated as follows: %MFI increase = (MFI with the given peptide – MFI without peptide) / (MFI without peptide) × 100.

Enzyme linked immunospot assay

Ninety-six-well plates (Millititer; Millipore, Bedford, MA) were coated with anti-human interferon-γ (IFN-γ) Ab Mabtech, Nacka, Sweden) at 4°C overnight and then washed 4 times with sterile PBS. The plates were next blocked with RPMI 1640 medium containing 5% FCS for 2 hr at 25°C. Three hundred thousand unfractionated PBMCs were added in duplicate cultures of RPMI 1640 containing 5% FCS together with the peptides at 10 μg/ml. After 24 hr, the plates were washed 8 times and incubated overnight with 100 μl of biotin conjugated anti-human IFN-γ Ab. After another 4 washes, streptavidin-AP was added for 2 hr. Finally, the plates were washed again 4 times with PBS and developed with freshly prepared NBT/BCIP solution (Biorad, Hercules, CA). The reaction was stopped by washing with distilled water, and after drying at room temperature, colored spots with fuzzy borders, which indicated the presence of IFN-γ secreting cells, were counted. The number of specific spots was determined by subtracting the number of spots in the absence of antigen from the number of spots in the presence of antigen. Responses were considered positive if more than 10 specific spots were detected and if the number of spots in the presence of antigen was at least twofold greater than the number of spots in the absence of antigen. Positive controls for IFN-γ enzyme linked immunospots (ELISPOTs) consisted of 10 ng/ml phorbol 12-myristate 13-acetate (Sigma), 500 ng/ml ionomycin (Sigma) or the HLA-A24-restricted EBV late membrane or CMV pp65-derived peptides (Table II).

Stimulation of PBMC with synthetic peptides

AFP-derived peptide-specific T cells were expanded from PBMCs in 96-well round bottom plates (NUNC, Naperville, IL) as previously described.[25] Briefly, 400,000 cells/well were stimulated with synthetic peptides at 10 μg/ml, 10 ng/ml rIL-7 and 100 pg/ml rIL-12 (Sigma) in RPMI 1640 supplemented with 10% heat inactivated human AB serum, 100 U/ml penicillin and 100 μg/ml streptomycin. The cultures were restimulated with 10 μg/ml peptide, 20 U/ml rIL-2 (Sigma) and 10^5 mytomicin C treated autologous PBMCs on days 7 and 14. On days 3, 10 and 17, 100 μl of RPMI with 10% human AB serum and 10 U/ml rIL-2 (final concentration) was added to each well.

Cytotoxicity assay

C1R-A24 cells, which are human lymphoblastoid HMYC1R cells transfected with the HLA-A*2402 molecule, and human hepatoma cell lines were used as target cells for CTL lines. C1R-A24 cells were incubated overnight with 10 μg/ml synthetic peptides and labeled with 25 μCi of ^{51}Cr (Amersham, Arlington Heights, IL) for 1 hr. Hepatoma cell lines were labeled with 25 μCi of ^{51}Cr for 1.5 hr without incubation with peptides. After 3 washes with PBS, the target cells were plated at 3,000 cells/well with complete medium in round-bottom 96-well plates. Unlabeled K562 cells at 120,000 cells/well were added to reduce nonspecific lysis. Stimulated PBMCs from patients were added at effector to target ratios of 100:1, 50:1, 25:1, 13:1, 6:1 and 3:1, respectively. For Ab-blocking assay, effector cells or ^{51}Cr-labeled target cells were preincubated with each monoclonal antibody (MAb) for 20 min at room temperature. The percent cytotoxicity was determined from the formula: 100 × [(experimental release − spontaneous release) / (maximum release − spontaneous release)], and maximum release was determined by lysis of ^{51}Cr-labeled targets with 5% Triton X-100 (Sigma Chemical). Spontaneous release was <15% of maximum release for all experiments. The specific cytotoxic activity was calculated as follows: (cytotoxic activity in the presence of peptide) − (cytotoxic activity in the absence of peptide).

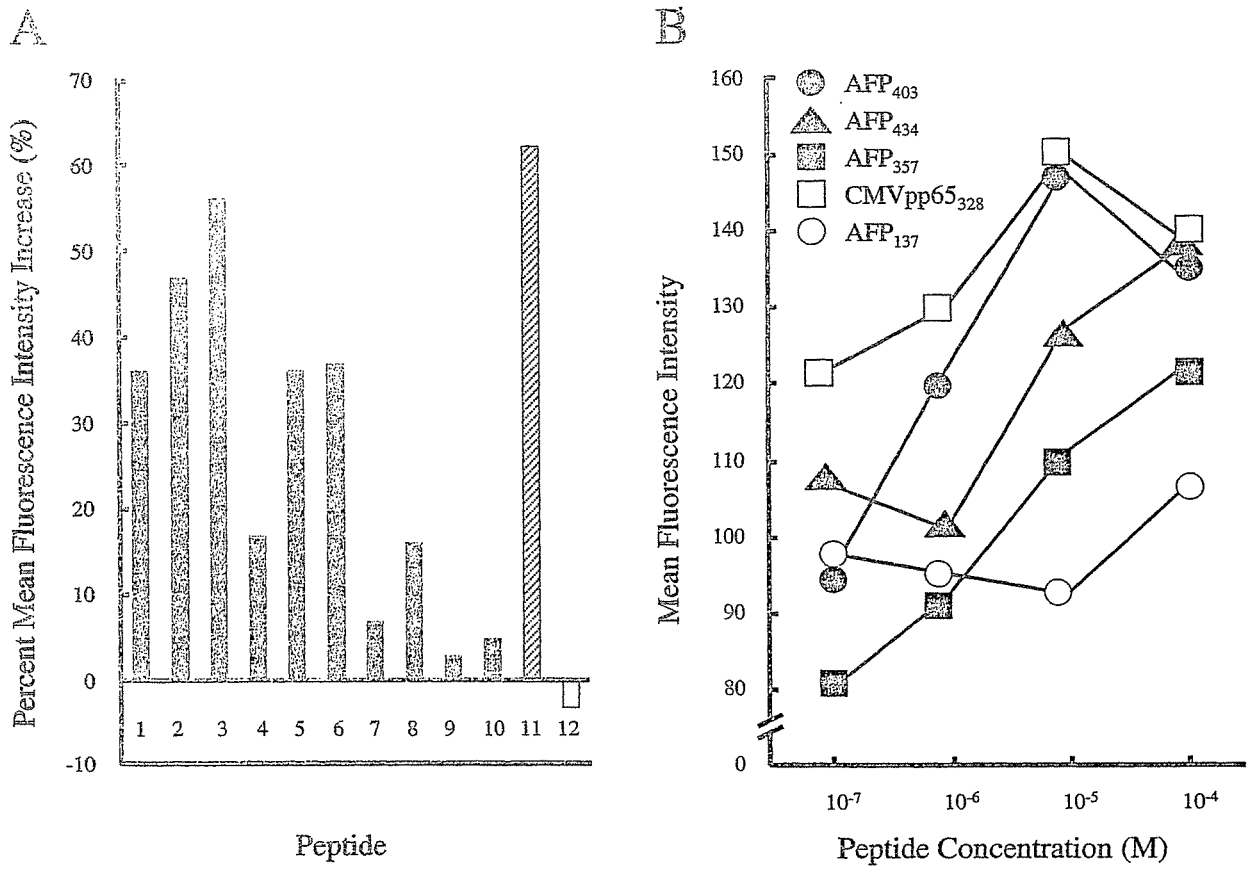

FIGURE 1 – MHC binding affinity. (*a*) TAP-deficient T2-A24 cells were cultured for 16 hr at 26°C to enhance the expression of peptide-receptive cell surface molecules. They were incubated with individual peptides at 10 μg/ml at 37°C for 2 hr, washed and stained with anti-HLA-A24 MAb, anti-mouse immunoglobulin conjugated FITC and 1 μg/ml of propidium iodide. The data are expressed as the %mean fluorescence intensity (MFI) increase for live, propidium iodide-negative cells. 1, AFP_{403}; 2, AFP_{424}; 3, AFP_{434}; 4, AFP_{357}; 5, AFP_{150}; 6, AFP_{504}; 7, AFP_{591}; 8, AFP_{414}; 9, AFP_{7}; 10, AFP_{322}; 11, $CMVpp65_{328}$; 12, AFP_{137}. (*b*) The MHC binding affinity of representative peptides is shown at various concentrations. The data are expressed as MFI for live, propidium iodide-negative cells.

Statistical analysis

Fisher's exact test (2-sided p-value) and the unpaired Student's *t*-test were used to analyze the effect of variables on immune responses in HCC patients.

Results

Patient profiles

The clinical profiles of the patients are shown in Table I. Thirty were positive for AFP ranging from 10 to 50,800 ng/ml. The tumors of 24 patients were histologically diagnosed as HCC, and their differentiation was well, moderate and poor for 11, 12 and 1 cases, respectively. Other tumors were diagnosed as being HCC by typical CT findings and AFP elevation. The tumor size was categorized as "small" ($\leqq$2cm) for 10 cases or "large" (>2cm) for 28 cases, and tumor multiplicity was categorized as "multiple" ($\geqq$2 nodules) for 23 cases or "solitary" (single nodule) for 15 cases. Vascular invasion of HCC was observed in 11 cases. The TNM stage was classified according to the Union Internationale Contre Le Cancer classification system (6th version),[26] where 13, 13, 5, 1, 2 or 4 patients had Stage I, II, IIIa, IIIb, IIIc or IV tumors, respectively. Thirty-seven patients received HCC treatment as described in Material and methods.

Selection of potential HLA-A24-binding peptides within AFP

To identify potential HLA-A24-binding peptides, the amino acid sequences of AFP were analyzed using a computer program designed to predict HLA-binding peptides (available at BIMAS website) based on the estimation of the half-time dissociation of the HLA-peptide complex. Ten peptides were selected according to the order of the high half-time dissociation scores (Table II). Next, MHC stabilization assays were performed to test these peptides for HLA-A*2402 binding capacity using T2-A24 cells. Most peptides increased HLA-A24 expression on the cells, indicating that they bound and stabilized the HLA complex on the cell surface except for peptides AFP_{591}, AFP_{7} and AFP_{322} (Fig. 1*a*). Peptide $CMVpp65_{328}$, which is identified as a strong binder of the HLA-A*2402 molecule,[22] increased HLA-A24 expression, but peptide AFP_{137}, which is HLA-A2 restricted,[14] did not increase the expression, suggesting that the assay was specific for HLA-A24.

To confirm these results, a HLA-A24 stabilization assay was performed at different concentrations using several representative peptides. As shown in Figure 1*b*, a positive control peptide and representative AFP-derived peptides increased HLA-A24 expression depending on the concentrations, but this did not occur for the HLA-A2-restricted peptide.

Immunogenicity of AFP peptides assessed by IFN-γ ELISPOT analysis

To determine whether these HLA-A24 binding peptides could be recognized by the T cells of patients with HCC, IFN-γ ELISPOT responses were evaluated with *ex vivo* PBMCs. Seven of 10 AFP-derived peptides were recognized by PBMCs of at least

1 patient, and 21 of 38 patients (55%) responded to at least 1 of the analyzed AFP-derived peptides.

An overview of all responses is shown in Figure 2*a*. Single AFP epitope-specific IFN-γ producing cells were detected in 5 (13.2%), 3 (7.9%), 8 (21.1%), 7 (18.4%), 2 (5.1%), 3 (7.9%) and 2 (5.1%) of the 38 patients for peptides AFP_{403}, AFP_{424}, AFP_{434}, AFP_{357}, AFP_{150}, AFP_{504} and AFP_{414}, respectively. Peptides AFP_{591}, AFP_{7} and AFP_{322} were not recognized by any patient. Among the peptides, AFP_{591}, AFP_{7} and AFP_{322} displayed a relatively low binding affinity for the HLA-A*2402 molecule compared with the other peptides (Fig. 1*a*). In contrast, peptides AFP_{403}, AFP_{434} and AFP_{357}, those with a high binding affinity for the HLA-A*2402 molecule, were recognized by 5, 8 and 7 patients, respectively. These data show that AFP-derived peptides with a high binding affinity for the HLA-A*2402 molecule were also immunogenic.

The strength of the AFP-specific T-cell responses assessed by the frequency of IFN-γ producing cells in the PBMC population is shown in Figure 2*a*. The maximum response was quantitated as 177 peptide-specific IFN-γ producing cells per 3×10^5 PBMCs. Most patients, however, displayed between 10 and 60 specific cells per 3×10^5 PBMCs. The frequency of positive T-cell responses was lower than that of peptides $EBVlm_{287}$ and $CMVpp65_{328}$, which were derived from EBV latent membrane or CMV pp65 protein, respectively, and are strongly immunogenic. All the patients who showed positive T-cell responses against $EBVlm_{287}$ or $CMVpp65_{328}$ were sero-positive for EBV or CMV, respectively. No patient exhibited positive T-cell responses against peptide $HIVenv_{584}$ derived from the HIV envelope protein, suggesting that these T-cell responses were antigen-specific.

In contrast to the results for the HCC patients, the ELISPOT assays for the normal donors did not show any IFN-γ producing cells against AFP-derived peptides (Fig. 2*b*), but the ratio of normal donors who showed positive T-cell responses for EBV or CMV protein-derived peptides and the frequency of T cells were not significantly different from those of the HCC patients (Fig. 2*b*). On the basis of these results, we selected peptides AFP_{403}, AFP_{424}, AFP_{434}, AFP_{357}, AFP_{150}, AFP_{504} and AFP_{414} as possible peptides that contain a $CD8^+$ T-cell epitope.

Identification of AFP-derived peptides that elicit a primary CTL response

The 7 selected AFP-derived peptides were tested for their potential to induce HLA-A24-restricted CTLs using the PBMCs from the HCC patients with HLA-A24. Each peptide was tested on at least three patients. After 3 rounds of stimulation, responder cells that had been stimulated with peptides AFP_{403}, AFP_{424}, AFP_{434}, AFP_{357} and AFP_{414} lysed the peptide-pulsed C1R-A*2402 cells as shown in Figure 3. On the other hand, other peptides, including those that showed binding affinity for the HLA-A24 molecule, failed to induce CTLs specific for the corresponding peptide. Thus, peptides AFP_{403}, AFP_{424}, AFP_{434}, AFP_{357} and AFP_{414} contained a HLA-A24 restricted AFP epitope.

Lysis of hepatoma cell lines by AFP peptide-specific CTL lines

We next determined whether AFP-derived peptide-induced CTLs showed cytotoxicity against hepatoma cell lines that produced AFP. As shown in Figure 4, peptides AFP_{403}- and AFP_{357}-specific CTLs showed cytotoxicity against HepG2, which expressed HLA-A*2402 and produced AFP, but not against HLE or HuH7, which lacked HLA-A*2402 expression or production of AFP.[27] These results indicate that the CTLs generated from PBMCs of HCC patients were able to kill hepatoma cells, and that the cytotoxicity was restricted by HLA-A24 and specific for AFP.

Furthermore, to confirm that the cytotoxicity was mediated by $CD8^+$ T cells and restricted HLA-A24, we examined the T-cell responses against peptide-pulsed C1R-A24 or HepG2 cells incubated with specific MAb. Anti-CD8 Mb and anti-HLA-A24 MAb efficiently inhibited the specific response of peptide AFP_{357}-induced CTLs against both cell types (Figs. 5*a* and 5*b*). Also, CTLs incubated without any Ab did not show cytotoxicity against K562 that did not express HLA molecules (Figs. 4*a* and 4*b*). Thus, we confirmed that the AFP-derived peptide-specific T-cell response was mediated by $CD8^+$ T cells and restricted by HLA-A24. In addition, together with the results of the ELISPOT assay, the data revealed that the peptide contains an epitope that is endogenously processed within the AFP producing cells.

AFP-specific T-cell responses and clinical features of HCC patients

To evaluate the status of AFP-specific T-cell responses in patients with HCC, we analyzed the relationships between the frequency of peptides AFP_{403}, AFP_{424}, AFP_{434}, AFP_{357} or AFP_{414}-specific T cells and the clinical features of patients by IFN-γ ELISPOT assay. AFP-specific IFN-γ producing cells in the peripheral blood were observed in 14 of the 30 (47%) patients with AFP-positive serum and were also observed in 4 of the 8 (50%) patients with AFP-negative serum. In 2 of the 4 patients who showed serum AFP negative but positive AFP-specific IFN-γ producing cells in the peripheral blood, serum AFP increased during the follow-up period. One out of the 4 patients could not be followed up because the patient had died. Thus, only 1 patient was confirmed to continuously have serum AFP below the detection limit during the follow-up period. In addition, analysis of the relationship between serum AFP levels and the positive rate of patients who had AFP-specific IFN-γ producing cells did not show a statistical correlation (Table III). These results suggest that the amount of AFP in serum is not associated with the induction of AFP-specific T cells.

Tumor factors indicated by the TNM classification (T2–T4 *vs.* T1) or TNM stage (Stage II–IV *vs.* Stage I) for the group with positive T-cell responses were significantly more advanced ($p = 0.006$) than those for the group without positive T-cell responses (Table III). Positive T-cell responses for the 5 peptides were observed in only 2 patients with TNM Stage I. Also, tumor multiplicity showed the same tendency between the 2 groups, although it was not significant. Differentiation of HCC, vascular invasion, histology of the nontumor liver, liver function and the type of viral infection were not associated with AFP-specific host immune responses (Table III).

Effect of anticancer treatment on AFP-specific T-cell responses

To analyze the effect of anticancer treatment on AFP-specific T-cell responses, we prospectively evaluated the T-cell responses for peptides AFP_{403}, AFP_{424}, AFP_{434}, AFP_{357} or AFP_{414} in 17 randomly selected patients undergoing HCC treatment. The frequency of AFP-specific T cells increased from 2 to 25 fold in 7 of the 17 patients after treatments (Fig. 6). In contrast, HIV-specific T-cell responses did not increase in all patients and CMV-specific T-cell responses increased in only 2 patients (Patients 14 and 31) (Fig. 6). These results suggest that the effect of anticancer treatment on the T-cell response is specific for AFP. The clinical profiles of the patients with or without increasing AFP-specific T-cell responsiveness after HCC treatment are shown in Table IV. The analyses of both patient groups showed that there were no differences in clinical factors except for the TNM stage. The ratio of

FIGURE 2 – Direct *ex vivo* analysis (IFN-γ ELISPOT assay) of peripheral blood T-cell responses to AFP-derived peptides (solid bars) or control peptides (open bars) in HCC patients (*a*) and normal donors (*b*). Only significant IFN-γ responses to at least 1of the 13 tested peptides are included in the figure. Responses were considered positive if more than 10 specific spots were detected and if the number of spots in the presence of antigen was at least twofold greater than the number of spots in the absence of antigen. The peptide sequences are described in Table II. The data for AFP_{591}, AFP_{7} and AFP_{322} are excluded because there was no positive T-cell response. * denotes 177 specific spots; **, 68 specific spots and ***, 92 specific spots.

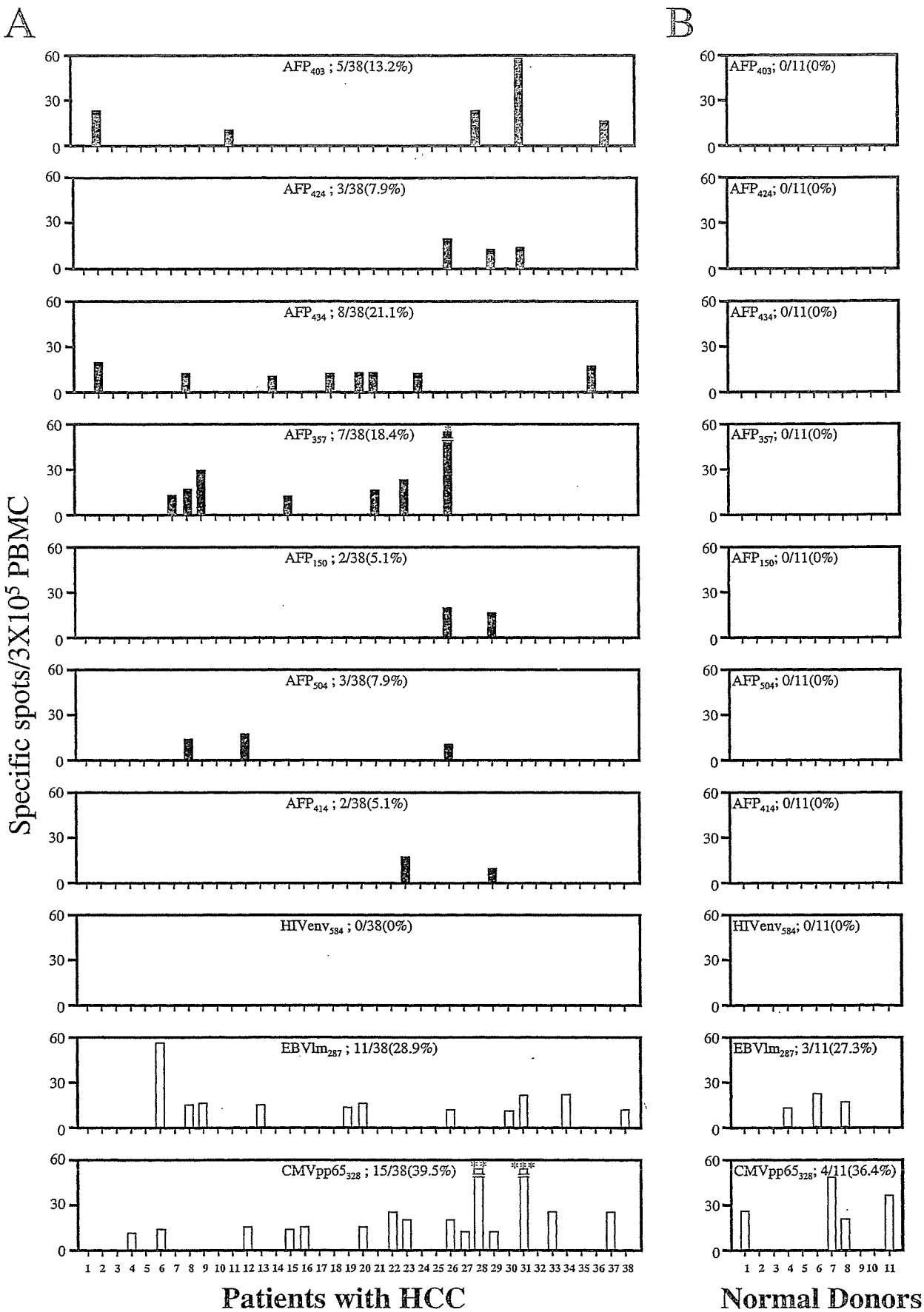
A
B
Specific spots/3X10^5 PBMC
AFP$_{403}$; 5/38(13.2%)
AFP$_{424}$; 3/38(7.9%)
AFP$_{434}$; 8/38(21.1%)
AFP$_{357}$; 7/38(18.4%)
AFP$_{150}$; 2/38(5.1%)
AFP$_{504}$; 3/38(7.9%)
AFP$_{414}$; 2/38(5.1%)
HIVenv$_{584}$; 0/38(0%)
EBVlm$_{287}$; 11/38(28.9%)
CMVpp65$_{328}$; 15/38(39.5%)
AFP$_{403}$; 0/11(0%)
AFP$_{424}$; 0/11(0%)
AFP$_{434}$; 0/11(0%)
AFP$_{357}$; 0/11(0%)
AFP$_{150}$; 0/11(0%)
AFP$_{504}$; 0/11(0%)
AFP$_{414}$; 0/11(0%)
HIVenv$_{584}$; 0/11(0%)
EBVlm$_{287}$; 3/11(27.3%)
CMVpp65$_{328}$; 4/11(36.4%)
0
30
60
1 2 3 4 5 6 7 8 9 10 11 12 13 14 15 16 17 18 19 20 21 22 23 24 25 26 27 28 29 30 31 32 33 34 35 36 37 38
1 2 3 4 5 6 7 8 9 10 11
Patients with HCC
Normal Donors

FIGURE 2.

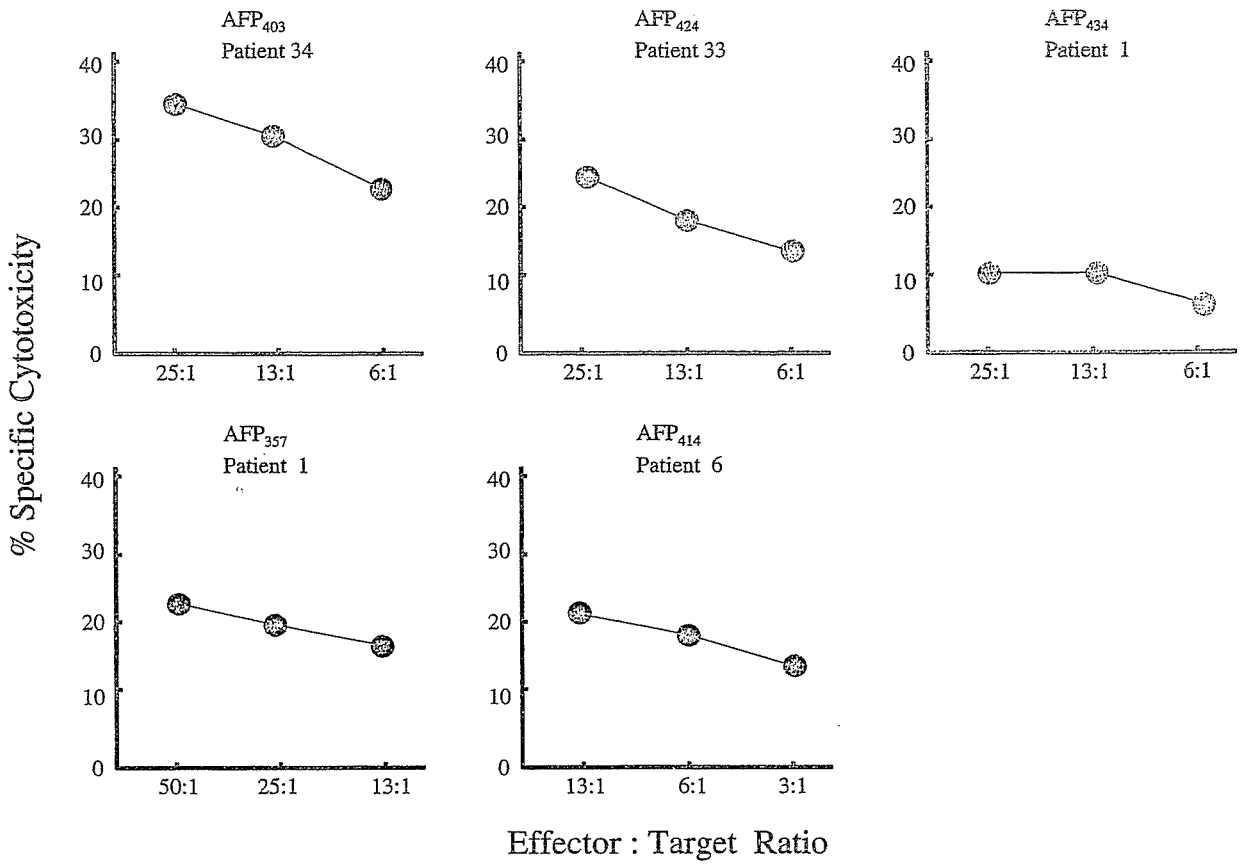

FIGURE 3 – Cytotoxicity of AFP-specific T-cell lines in patients with HCC. The cytotoxicity of the T-cell lines was determined by a standard 6 hr cytotoxicity assay at various effector to target (E/T) ratios against C1R-A*2402 cells pulsed with 1of the AFP-derived peptides listed in Table II. The number of patients corresponds to the numbers as shown in Table I. The data are indicated as the percent specific cytotoxicity, which is calculated as follows: (cytotoxicity in the presence of specific peptide) – (cytotoxicity in the absence of peptide).

patients with TNM Stage I or II was greater for patients with increasing T-cell responsiveness than for those without (Table IV). Furthermore, 5 of the 7 patients who showed increasing AFP-specific T-cell responsiveness after HCC treatment did not show a response before treatment.

Discussion

AFP is a sugar-containing protein ~70 kDa in molecular weight[28] and is produced at high levels by the yolk sac and fetal liver. In adults, AFP is produced by 80% of HCC and certain germ cell tumors, and production increases in benign liver diseases such as chronic hepatitis and cirrhosis.[29,30] Furthermore, the expression of AFP in cancerous tissue is related to the biological malignancy of HCC.[31] Recent studies reported that AFP-specific T-cell clones are not deleted during ontogeny and that AFP is recognized by murine[16] and human T cells[13–15] and serves as a tumor rejection antigen in a murine tumor model.[16] Therefore, AFP has the potential of being a target of immunotherapy for HCC. However, the number of AFP epitopes that have been identified is limited and the status of AFP-specific immunological responses has not been well-characterized for patients with HCC. To address this issue, we tried to identify HLA-A*2402-restricted T-cell epitopes derived from AFP and to analyze the relationship between AFP-specific immunological responses and clinical features in HCC patients.

First, we attempted to identify AFP epitopes restricted by HLA-A24 that are present in 60 % of Japanese, 20% of Caucasians and 12% of Africans,[32,33] using a combined computer-based and immunological approach. Analysis of amino acid sequences of AFP by computer revealed a number of potential HLA-A24-binding peptides, and most of them functionally stabilized HLA-A*2402 molecules expressed in the peptide transporter-deficient cell line T2-A24. Five AFP-derived peptides (Peptides AFP_{403}, AFP_{424}, AFP_{434}, AFP_{357} and AFP_{414}) showing HLA-A*2402 binding affinity induced IFN-γ production of PBMCs and T-cell lines that showed cytotoxicity against the peptide-pulsed C1R-A24 cells. In addition, these T-cell lines showed cytotoxicity against hepatoma cell lines that expressed HLA-A*2402 and AFP, but did not show it against other hepatoma cell lines without HLA-A*2402 or AFP expression, suggesting that the cytotoxicity was HLA-A24-restricted and AFP-specific. Taken together with the result that cytotoxicity was inhibited by incubation with anti-CD8 Mb and anti-HLA-A24 MAb, we confirmed that the 5 peptides contained HLA-A24-restricted AFP epitopes that were endogenously processed within the AFP producing cells.

To study the status of host immunological responses to AFP in HCC patients, we examined the frequency of AFP-specific T cells in the peripheral blood by ELISPOT assay with the 5 epitopes, and analyzed the relationships between the frequency and the clinical features of the patients. ELISPOT assay showed that the frequency of reactive T cells to a single AFP epitope was 30–190 per 1×10^6 PBMCs. On the other hand, ELISPOT assay using HIV envelope-derived peptide did not show any positive T-cell responses. In addition, all the patients who showed positive T-cell responses against $EBVlm_{287}$ or $CMVpp65_{328}$ were sero-positive

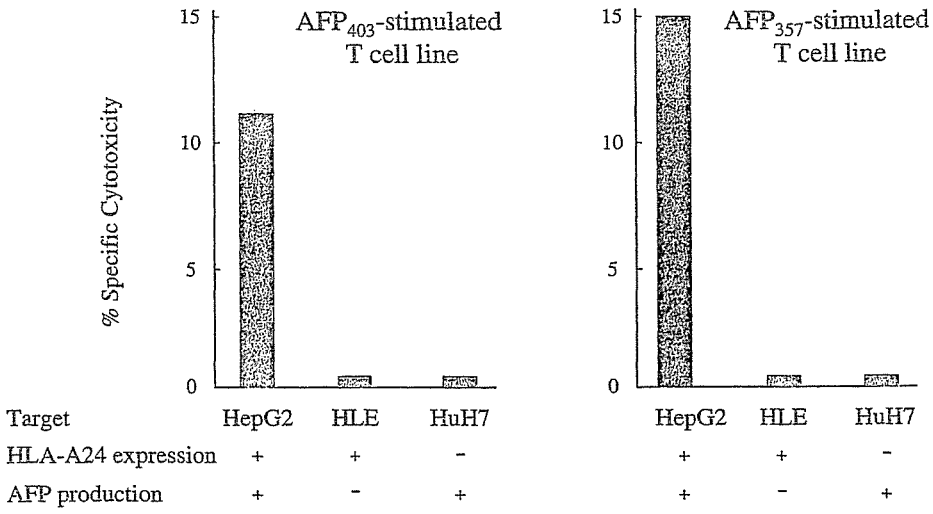

FIGURE 4 – Cytotoxicity of AFP-specific T-cell lines on cancer cell lines that do or do not express HLA-A*2402 or AFP. The cytotoxicity was determined by a standard 6 hr cytotoxic assay (E/T ratio of 50:1).

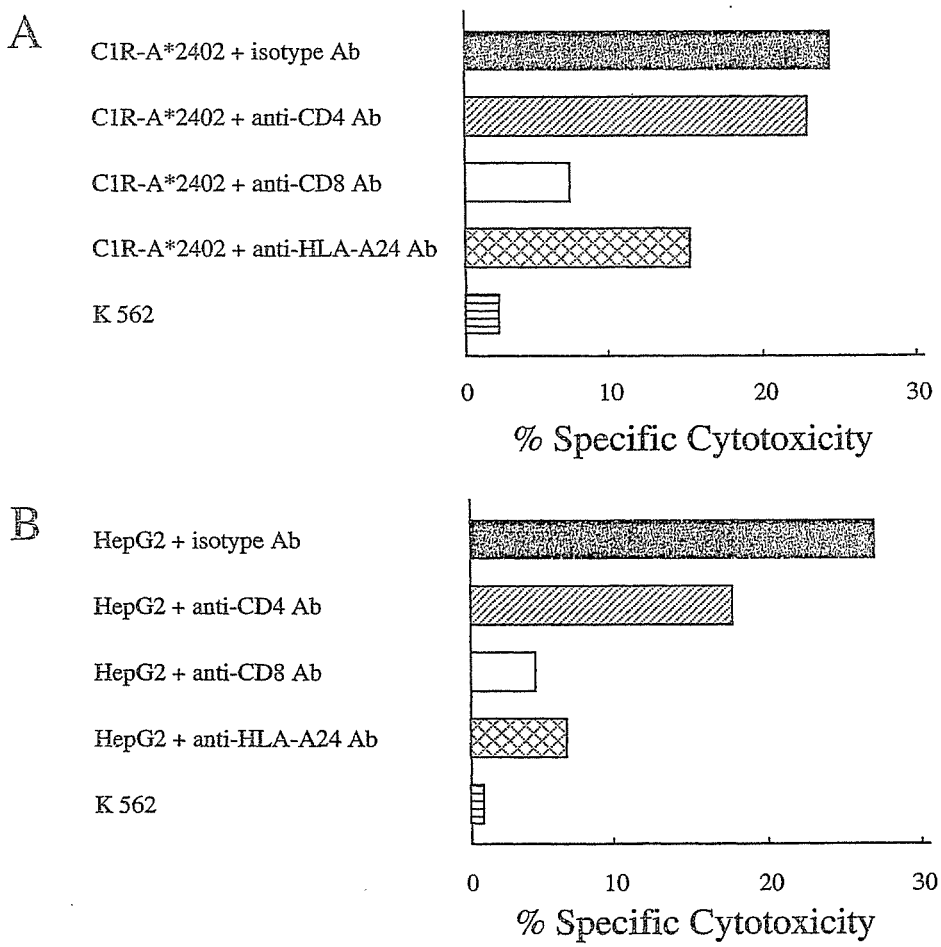

FIGURE 5 – Inhibition of cytotoxicity of AFP-specific T-cell lines by specific antibodies. T-cell lines were generated from PBMC of HCC patients by stimulation with AFP_{357}. Inhibition of cytotoxicity was determined using a standard 6 hr cytotoxicity assay against C1R-A*2402 cells pulsed with AFP_{357} (*a*) or HepG2 cells (*b*) incubated with anti-CD4, -CD8 or -HLA-A24 MAbs (E/T ratio, (*a*) 50:1; (*b*) 20:1). Cytotoxicity of AFP-specific T-cell lines against K562 cells was also examined for the same E/T ratio.

for EBV or CMV, respectively. These results suggest that the ELISPOT responses are correlated with their serological results and these peptides may be recall antigens. In previous reports regarding the frequency of T cells specific for a single tumor associated antigen epitope, the number of specific T cells for tyrosinase, MelanA/MART-1, gp100 or CEA in patients with melanoma or colorectal cancer was found to be 11–130 per 1×10^6 PBMCs.[34,35] In addition, single AFP epitope-specific IFN-γ producing cells were detected in 5.1–21.1% of the patients for peptides AFP_{403}, AFP_{424}, AFP_{434}, AFP_{357} or AFP_{414}. These rates are similar to previously reported epitopes for tyrosinase, MelanA/MART-1, gp100, Her-2/neu and CEA.[34–39] Comparing the present